Early life stress-induced miR-708-5p affects bipolar disorder-associated phenotypes through neuronatin downregulation.

Carlotta Gilardi[1], Helena C. Martins[1], Alessandra Lo Bianco[1], Silvia Bicker[1], Pierre-Luc Germain[1, 2, 3], Fridolin Gross[1*], Ayse Özge Sungur[4,5,6,7], Theresa M. Kisko[4,5,6,7], Frederike Stein[8], Susanne Meinert[9], Rainer K. W. Schwarting[4], Markus Wöhr[4,5,6,7], Udo Dannlowski[9], Tilo Kircher[8], and Gerhard Schratt[1§]

1 ETH Zurich, Lab of Systems Neuroscience, Institute for Neuroscience, Department of Health Science and Technology, 8057 Zurich, Switzerland

2 Laboratory of Molecular and Behavioural Neuroscience, Institute for Neuroscience,

Department of Health Science and Technology, ETH Zürich, Switzerland

3 Lab of Statistical Bioinformatics, IMLS, University of Zürich, Switzerland

4 Philipps-University of Marburg, Faculty of Psychology, Experimental and Biological Psychology, Behavioral Neuroscience, D-35032 Marburg, Germany

5 Center for Mind, Brain and Behavior, D-35032 Marburg, Germany

6 KU Leuven, Faculty of Psychology and Educational Sciences, Research Unit Brain and Cognition, Laboratory of Biological Psychology, Social and Affective Neuroscience Research Group, B-3000 Leuven, Belgium.

7 KU Leuven, Leuven Brain Institute, B-3000 Leuven, Belgium

8 Department of Psychiatry and Psychotherapy, University of Marburg, Marburg, Germany.

9 Institute for Translational Psychiatry, University of Münster, Münster, Germany.

*current address: CNRS UMR5164 ImmunoConcEpT, University of Bordeaux, France

§: to whom correspondence should be addressed: Gerhard.schratt@hest.ethz.ch

Running title: miR-708-5p in bipolar disorder

Abstract

The underlying physiological and molecular mechanisms of bipolar disorder (BD) remain largely unknown. Here, by using unbiased small RNA sequencing in peripheral blood mononuclear cells (PBMCs), we found that miR-708-5p, a microRNA that was previously associated with BD, is the most strongly upregulated microRNA in peripheral blood of both healthy human subjects with a high genetic or environmental predisposition to develop mood disorders (MDs). Furthermore, miR-708-5p is strongly upregulated in patients diagnosed with BD and has potential in conjunction with the previously identified miR-499-5p to differentiate BD patients from patients suffering from major depressive disorder (MDD) and healthy controls. miR-708 is also upregulated in the hippocampus of wild type juvenile rats that underwent social isolation, as well as in juvenile rats heterozygous for the BD risk gene *Cacna1c*. Furthermore, ectopic overexpression of miR-708-5p in the hippocampus of adult male mice leads to BD-associated endophenotypes, such as reduced behavioral despair, enhanced compulsivity, and short-term memory impairments. miR-708-5p directly targets Neuronatin (Nnat), an endoplasmic reticulum (ER) resident protein involved in calcium homeostasis. Restoring Nnat expression in the hippocampus of miR-708-5p overexpressing mice rescues BD-associated endophenotypes. In summary, we functionally link miR-708-5p dependent regulation of Nnat to BD, with potential implications for BD diagnosis and therapy.

Introduction

MDs are a group of chronic psychiatric diseases affecting mood and cognition that include Major Depressive Disorder (MDD) and Bipolar Disorder (BD). MDD is characterized by long, persistent, depressive episodes. BD has a distinct pattern of mood oscillations, from depressive episodes like MDD, and (hypo)manic phases. Furthermore, BD is subclassified in BD type 1 (mania and depression), and BD type 2 (hypomania and depression). It is known that MDs are highly heritable and share common genetic signature (1). In particular, BD is characterized by up to 70% heritability in monozygotic twins (2). However, complex polygenetic mechanisms cannot fully explain the onset of BD, and environmental factors, such as early life stress, play an important role in the etiology and outcome of BD (3–5). Furthermore, BD presents sex-specific mood and cognitive features. Manic episode onset occurs earlier in life in men (6,7), while women experience more depressive episodes (6). From the cognitive side, men perform worse in recognition memory tasks than women, but they do better in working memory tests (8).

Preclinical studies have employed genetic and environmental animal models of BD, most of them mimicking the manic or the depressive phase of the disease. Several environmental and genetic mouse models, e.g., sleep deprivation (9), deficiency of the circadian regulator *Clock* (10) or the cytoskeleton regulator *Ank3* (ANK-G) (11), recapitulate aspects of the manic endophenotypes of BD. They display reduced immobility in the forced swim test (FST), an effect which models reduced helplessness and antidepressant-like behavior. Furthermore, they show reduced anxiety in the open field test (OFT), and higher preference for reward stimuli and hedonic behavior (sucrose, cocaine) (10). Similarly, when the lithium target GSK3β is pharmacologically inhibited, mice show no mania-like behavior in the amphetamine-induced hyperactivity test (12). Mice haplo-insufficient for the cross-psychiatric risk gene *Cacna1c* show decreased immobility in the tail suspension test (TST) and FST, higher preference for sucrose as well as decreased anxiety behavior, although the latter was a characteristic of female mice only (13).

Recent research has highlighted the role of microRNAs (miRNAs) in the pathogenesis and their potential for treatment of MDs, including BD (14). miRNAs are a large family

of small (~22nt), noncoding RNAs that act as posttranscriptional regulators by binding to complementary sequences in the 3′- untranslated region (UTR) of target messenger RNAs (mRNAs) (15). miRNAs are widely expressed in the brain, where they regulate neuroplasticity (16) and cellular stress responses (17). They have been associated with BD etiology in expression studies of postmortem brain tissue of BD patients (18). Furthermore, lithium and valproic acid (VPA), the primary mood stabilizers used in BD treatment, affect miRNA expression (19,20). Variants in miRNA genes associated with a higher risk of BD have been identified (21), and manipulation of one of these miRNAs (miR-499-5p) caused cognitive impairments and mood disorder-related endophenotypes in rats (14,22). However, most miRNAs dysregulated in BD have not been functionally investigated, and the molecular mechanisms by which they control BD-associated endophenotypes remain largely unknown. Differential expression of miRNAs in peripheral blood mononuclear cells (PBMCs) has been often investigated for biomarker discovery in psychiatric disorders. For example, miR-499-5p was significantly upregulated in female and male PBMC samples of BD (22). miR-124-3p was found to be significantly upregulated in PBMCs samples of MDD compared to healthy controls and it was downregulated after eight weeks of antidepressant treatment (23). miR-30a-5p was downregulated in the PBMCs of unmedicated patients in acute state schizophrenia (SCZ) and upregulated following antipsychotic treatment (24). However, these attempts so far have not yielded reliable miRNA biomarkers in MDs, especially regarding the differential diagnosis of BD and MDD.

In this study, we identified miRNA-708-5p as a miRNA whose expression is induced by genetic and environmental risk in rats and humans. Previous studies already pointed to a potential role of miR-708-5p in the development of MDs. miR-708-5p is nominally associated with BD in GWAS (21) and it originates from the first intron of *ODZ4*, a protein-coding gene which is also significantly associated with BD (25). Moreover, both *ODZ4* and miR-708-5p expression are stress susceptible (26–28). It was shown that the synthetic glucocorticoid dexamethasone (DEX) upregulates *ODZ4* and miR-708-5p in the context of ovarian cancer (29). Moreover, CCAAT/enhancer binding protein (C/EBP) homologous protein (CHOP) can induce *ODZ4* and miR-708-5p expression upon ER stress activation (30). A recent study

reported miR-708-5p upregulation in the PFC upon seven days of chronic social defeat in vulnerable rats compared to resilient animals (31).

Neuronatin (Nnat) was previously identified as a target of miR-708-5p (26,28,32–34). It is a small protein bound to the Endoplasmic Reticulum (ER) membrane that antagonizes the activity of sarco-endoplasmic reticulum calcium ATPase (SERCA), thereby regulating calcium re-uptake from the cytosol to the ER (35,36). In neurons, Nnat controls dendritic calcium transients (32) and intracellular calcium levels in the context of Angelman syndrome (33). Intriguingly, both ER stress (37) and dysregulated calcium homeostasis (38) have been repeatedly linked to BD. The importance of the miR-708-5p/Nnat pathway for MDs, however, has not yet been investigated.

Materials and Methods

Human study

Recruitment of Participants

The study involved participants with BD (26 females, 37 males), MDD (18 females, 24 males), and healthy individuals (26 females, 31 males), including psychiatrically healthy subjects that had a history of childhood maltreatment (17) or a genetic predisposition to MDs (18) or no risk (18). MDsThese participants were recruited from the University of Marburg and the University of Münster in Germany, as part of the FOR2107 cohort (39). Diagnoses were made using the SCID-I interview (40), and adapted to DSM-IV criteria (41), excluding those with substance abuse, severe neurological, or other significant medical conditions. Healthy controls were screened similarly, with inclusion in the maltreatment study if at least one of the subclasses of the Childhood Trauma Questionnaire (CTQ) reached the maltreatment threshold (Emotional Abuse ≥ 10, Physical Abuse ≥ 8, Sexual Abuse ≥ 8, Emotional Neglect ≥ 15, and Physical Neglect ≥ 8) (42). All participants underwent a comprehensive neuropsychological test battery, including the d2 test of attention (43). All necessary ethical approvals were obtained (ethics committees of the Medical Faculties of the Universities of Münster (2014-422-b-S) and Marburg (AZ: 07/14)), and participants consented to the study, which complied with the Declaration of Helsinki and the Belmont Report. Demographic and clinical data are outlined in Table 1 and in Supplementary Table 1.

Human peripheral blood mononuclear cell (PBMC) sample processing.

PBMCs were obtained from 10 ml of whole blood using the LeukoLOCK technology (Thermo Scientific) at the Biomaterialbank Marburg, Germany. After sample randomization, total RNA extraction from PBMCs was carried out using the *mir*Vana™ kit (Thermo Fisher) or TRIzol™ Reagent (Thermo Fisher) following the manufacturer's protocol.

PBMCs processing for small RNA-sequencing

For the Small RNA-sequencing, RNA was extracted with *mir*Vana™ kit (Thermo Fisher) and DNase treated, and it was carried out at Functional Genomic Center Zurich (FGCZ, https://fgcz.ch/).

Small RNA-analysis

Short RNA reads were processed using the ncPro 1.6.4 pipeline (44) using the hg19 annotated (based on miRBase version 21). Only mature miRNA reads (accepting +2bp on either end) were considered for downstream analysis. Differential expression analysis was then performed using limma/voom 3.46.0 (45), with a model including a covariate to correct for the two technical batches.

Rat primary neuron culture

Cultures of primary hippocampal and cortical neurons from rat hippocampus were established using E18 Sprague-Dawley rats obtained from Janvier Laboratories, as described previously (22).

Transfection

Primary hippocampal neurons were transfected with Lipofectamine™ 2000 Reagent and plasmid DNA constructs as previously described (22).

Virus infection

Primary hippocampal neurons were infected with recombinant adeno-associated virus (rAAV) containing hpCTL or hp708 constructs on *days in vitro* (DIV) 2 by adding 300µl of a mixture of the virus with 300µl of NBP+ per well of a 24-well plate. Cells were used for downstream analysis on DIV19-20.

Luciferase Assay

DIV6 hippocampal neurons were transfected with 100ng of the Nnat-3'UTR luciferase reporters and 500ng of hpCTL-p or hp708-p, spCTL-p or sp708-p. After seven days from transfection, the cells were lysed, luciferase assay was conducted using a GloMax R96 Microplate Luminometer (Promega), as previously described (22). The relative luciferase activity was determined by calculating the ratio of the Firefly signal to the Renilla signal.

In Situ Hybridization

Single-molecule fluorescence *in situ* hybridization (smFISH) for miRNA detection in hippocampal neuron cultures was conducted using the QuantiGene ViewRNA miRNA Cell Assay Kit (Thermo Fisher, QVCM0001) following the manufacturer protocol with minor adjustments. Probes for has-miR-708-5p (Alexa Fluor 546, Thermo Fisher), Nnat (Alexa Fluor 546), CamK2 (Alexa Fluor 488) and Gad2 (Alexa Fluor 488) were used for the assay.

Plasmid design and rAAVs preparation

For rAAV-mediated overexpression of miR-708-5p, the chimeric miR-708 hairpin was generated by polynucleotide cloning. A detailed description and characterization of this system have been published (14,46). To knockdown miR-708-5p, a sponge plasmid was constructed by inserting six TDMD sites predicted to bind miR-708-5p in the 3'UTR of eGFP on rAAV-hSyn-EGFP. To perform luciferase activity analysis, the wild type and mutated Nnat 3'UTR was inserted into a pmirGLO dual-luciferase expression vector (Promega). Detailed description of the design of these constructs and of the rescue constructs are listed in the supplementary material section. Viral vectors were produced by the Viral Vector Facility (VVF) of the Neuroscience Center Zurich (https://www.vvf.uzh.ch).

Animal studies

Mouse experiments

Husbandry, housing, and behavioral testing

All animal experiments on mice were conducted in accordance with Switzerland's animal protection laws and received approval from local cantonal authorities (Approval ID: ZH194/21). Mice were housed collectively in cages designed for 2 to 4 individuals, with unrestricted access to food and water. The animal facility maintained an inverted light-dark cycle of 12 hours, with behavioral assessments conducted during the dark phase. Prior to experimentation, mice underwent daily handling lasting 5 minutes each over one week. Details about general behavioral procedures can be found in the supplementary materials and methods section.

Stereotactic surgeries and post-operative care

Stereotactic brain injections were conducted on 3-month-old C57BL/6JRj wild-type mice. The mice were anesthetized with 5% isoflurane in oxygen (1 L/min) and positioned on a stereotactic frame. Viral injections were carried out bilaterally. For dorsal hippocampus, the coordinates used were AP: -2.1mm; ML: ±1.5mm. For ventral hippocampus, the coordinates used were AP: -3.3mm; ML: ±2.7mm. Detailed description of the procedure and post-operative care can be found in the supplementary materials and methods section.

Open Field Test

Mice were placed in an open field box (size: L 45 x W 45 x H 40 cm, TSE System, Bad Homburg, Germany) with a 60-minute exploration window. Dim, yellow light was used in the Open field test of Supplementary Fig. 4H and I, and Supplementary Fig. 6C, D, E. 30 lux, white light was used for the Open Field in Supplementary Fig. 4J. The experiment was recorded, and the TSE VideoMot2 analyzer software (TSE Systems, Bad Homburg, Germany) was used for the automated assessment.

Elevated Plus Maze Test

The mouse was placed on the center of the elevated plus maze, a cross-shaped apparatus with two open arms and two closed arms, each arm measuring L 65 x W 5.5 cm and elevated 62 cm from the ground. 20 lux white light was used. Behavior was recorded on video for five minutes. The videos were automatically analyzed using TSE VideoMot2 analyzer software (TSE Systems, Bad Homburg, Germany)

Saccharin Preference Test

Mice were habituated in their standard group housing to the presence of two bottles for 48 hours before the test. The test was performed by single housing the test animals, and two bottles of tap water or 0.1% Saccharin solution were given to them for 48 hours. The weight of the bottles was recorded at the beginning of the test and every 12 hours around the light change (09:00-09:15 am/pm). The position of the bottle was exchanged each time to avoid side preference. The animals were re-grouped after the test ended.

Novel Object Recognition (NOR) Test

The test was performed as previously described (47), with slight modifications: 1. Twenty-four hours prior to testing, the animals were habituated to the arena used for

the test; 2. The break between familiarization and novelty introduction rounds was extended to five minutes or 24 hours.

Marble Burying Test

The test was conducted as previously described (48).

Passive Avoidance Test

The test was conducted using the Passive Avoidance 2-Compartment light-dark arena of the TSE System. The white light was set to 500 lux. On day one, the animal was placed into the light compartment while the door to the dark one wass open and it was allowed to explore; once it passed to the dark compartment, the door closed, and the animal received a 2-seconds foot shock of 0.3 mA after three seconds. On day two, the animal was placed again into the light compartment and, after 15 seconds, the door was automatically opened. The latency to enter the dark compartment was measured.

Tail Suspension Test

The mouse was hung by its tail for a duration of six minutes using a piece of tape affixed to the suspension metal bar, elevated approximately 50 cm from the ground. Before initiating the experiment, a climb-stopper, following the procedure outlined by Can and colleagues(49), was placed at the mouse tail base to prevent climbing. The sessions were recorded on video, and the duration of immobility was subsequently quantified.

Tissue collection

Animals were sacrificed by cervical dislocation and the hippocampus was collected on an ice-cold glass plate and subsequentially snap-frozen for RNA extraction (Trizol protocol) and gene expression analysis or for histological assessments after 4% paraformaldehyde fixation, cryoprotection through 30% sucrose solution, and coronal sectioning at the cryostat. Further details can be found in the supplementary materials and methods section.

Rat experiments

All animal experiments on rats were conducted in accordance with the National Institutes of Health Guidelines for the Care and Use of Laboratory Animals and were subject to prior authorization by the local government (MR 20/35 Nr. 19/2014 and

G48/2019; Tierschutzbehörde, Regierungspräsdium Giessen, Germany). Constitutive heterozygous *Cacna1c*$^{+/-}$ animal breeding and the juvenile social isolation paradigm were conducted as described in (22).

RT-qPCR

Total RNA extraction from mouse brain tissue, PBMC samples, and primary hippocampal cultures was performed using TRIzol™ Reagent (Thermo Fisher, 15596026), and total RNA was subsequently extracted following the manufacturer's guidelines. Further details can be found in the supplementary materials and methods section.

PolyA RNA sequencing sample preparation

Total RNA extraction from mouse hippocampus was extracted TRIzol™ Reagent (Thermo Fisher, 15596026). The RNA was then treated with Turbo DNase enzyme. 600 ng of DNase-treated RNA was used for High Throughput Transcriptome sequencing. Libraries were prepared with Illumina TrueSeq mRNA protocol and the transcriptome sequencing was run on Illumina Novaseq 6000. The transcriptome sequencing was carried out by the Functional Genomic Center Zurich (FGCZ, hyperlink: https://fgcz.ch/).

PolyA RNA sequencing analysis

Reads were mapped to the GRCm39 genome with STAR 2.7.8a (50) using the GENCODE M26 annotation as reference and quantified at the gene-level using featureCounts 1.6.4 (51). Genes were filtered using edgeR's filterByExpr function before differential expression analysis with edgeR 3.32.1 (52) using likelihood ratio tests with 3 surrogate variables estimated using sva 3.38.0 (53). TargetScan 7 (54)was used to predict miRNA targets. For gene expression across different brain cell types (Figure 4B), the Allen 10X+smartSeq taxonomy and per-cluster expression was used, aggregating non-neuronal cell types into broader classes.

Western blot

Proteins from primary hippocampal neurons were isolated using ice cold RIPA lysis buffer. 20ug of protein was mixed with 4xLaemmli Sample Buffer (Biorad) and were run on a 4–20% Mini-PROTEAN® TGX™ Precast Protein Gels (Biorad). Proteins were

transferred on a nitrocellulose membrane and blocked for two hours at room temperature in blocking solution and incubated in primary antibody solution for 48 hours at 4°C. Membranes were washed and incubated with secondary antibody for 1h. Membranes were washed five times in TBS-T, developed with the Clarity™ Western ECL Substrate (Bio-Rad) and visualized with the ChemiDocTM MP, Imaging System (BioRad). Further details can be found in the supplementary materials and methods section.

Statistical analysis

Details regarding the statistical analysis are listed in the Supplementary Materials and methods section.

Results

miR-708-5p is upregulated in the peripheral blood of human subjects at risk for or diagnosed with MDs.

miRNAs have been associated with MDs, but their functional role in the development of such disorders is still largely unexplored (14). To identify candidate miRNAs, we performed small-RNA sequencing with total RNA obtained from peripheral blood mononuclear cells (PBMCs) of healthy subjects (n=52) from the FOR2107 cohort (39) characterized by a high genetic (at least one first degree relative diagnosed with a mood disorder; GR group; n=14) or environmental (ER group; childhood trauma based on childhood trauma questionnaire (CTQ) score; n=16) predisposition to develop MDs (Fig. 1A; Table 1). For this initial analysis, we selected females since we were able to form more homogeneous GR and ER groups with females compared to males. We then focused on miRNAs that were differentially expressed in both ER and GR compared to healthy control subjects (CTL group; no known genetic or environmental risk factors; n=18), reasoning that such miRNAs would represent strong candidates for being functionally involved in MDs. We found that a total of six miRNAs (miR-412-5p, miR-100-5p, miR-501-3p, miR-642a-5p, miR-4999-5p, miR-708-5p) fulfilled this criterium (Fig. 1B and C). Among them miR-708-5p was of specific interest, since it was the most strongly upregulated miRNA. It was previously

shown to be induced by various forms of cellular stress (26–30) and had been associated with BD in the past (21). We could confirm that miR-708-5p is significantly upregulated in the GR and ER groups using qPCR (Fig. 1D).

Given these results, we speculated that miR-708-5p could also be altered in PBMCs of patients diagnosed with MDD or BD. Therefore, we assessed the levels of miR-708-5p in PBMCs obtained from MDD (n=42) and BD (n=63) patients (Fig. 1A; Table 1) by qPCR. miR-708-5p was significantly upregulated in female BD (n=26) and MDD (n=18) patients (Fig. 1E) compared to CTL (n=26), after correcting for age and antidepressant treatment (Fig. S1A-B), whereby the effect was more pronounced in BD compared to MDD patients. A similar picture was observed in male patients. Here, the increase was highly significant for BD subjects (Fig. 1F), after age and antidepressant treatment correction (Fig. S1C), and only trending for patients affected by MDD (Fig. 1F, Fig. S1D). Furthermore, miR-708-5p was significantly upregulated in both subtypes of BD in both female (Fig. S1E) and male (Fig. S1F) subjects. In female subjects, the only significant BD state for miR-708-5p upregulation was mania, although it only included two samples (Fig. S1G). There was also a significant miR-708-5p upregulation in depressive and hypomanic states in male subjects (Fig. S1H).

miR-708-5p levels showed a trending positive correlation with the Young Mania Rating Scale (YMRS), which is used to assess manic-like symptomatology in subjects affected by BD (Fig. 1G). In contrast, miR-708-5p did not show any correlation with YMRS in female subjects affected by BD (Fig. 1H). We also investigated whether miR-708-5p correlated with the Beck's depression inventory (BDI), in MDD male and female subjects, but no significant or trending correlation could be observed (Fig. S1I and J). Taken together, our results suggest that miR-708-5p is elevated in the peripheral blood of mood disorder patients, with a particularly strong upregulation observed for BD males.

We then asked if miR-708-5p was also differentially expressed in PBMCs obtained from patients suffering from related psychiatric disorders. For that purpose, we chose schizophrenia (SCZ), given the high genetic similarities between SCZ and BD (55). We performed qPCR on PBMCs from female (n=8) and male (n=15) SCZ

patients but were unable to detect any significant change in miR-708-5p expression compared to healthy control subjects (CTL; n=19) (Fig. S1K).

One of the biggest challenges in mood disorder diagnostics is to distinguish BD and MDD patients, especially when BD patients are in a depressive phase (56,57). Given our results from Fig. 1D-H, we hypothesized that miR-708-5p expression in PBMCs could be used as a diagnostic tool to classify samples into BD or control group, and BD or Control and MDD group. To do this, we performed receiver operating characteristic (ROC) curve analysis (58) and used miR-708-5p expression as predictor variable. We found that miR-708-5p alone performed better in male samples than in female samples when asked to discriminate BD patients from controls and MDD patients (Fig S2A and B), consistent with our previous results (Fig. 1 D-H). We then performed the same analysis using the expression values of miR-499a-5p, which we previously found to be significantly upregulated in male BD subjects compared to healthy controls (22). Like miR-708-5p, miR-499a-5p performed better as a classifier in male subjects compared to female subjects (Fig S2C and D). Furthermore, we performed another ROC curve analysis considering both miRNAs together and found that the combined expression of miR-708-5p and miR-499a-5p performs better (AUC=0.908) in classifying male BD vs controls and MDD (Fig. 1I) than when the miRNAs are analyzed individually. In addition, the combination performs better (AUC=0.914) also in classifying male BD vs controls (AUC=0.914) (Fig S2E).

Taken together, our results show that the combined expression of miR-708-5p and miR-499a-5p in PBMCs shows a good predictive potential to distinguish BD patients from MDD patients and healthy controls, in particular regarding males.

miR-708-5p is expressed in rat hippocampal neurons and upregulated in the hippocampus of rat models of environmental or genetic risk for MDs.

To further study the functional role of miR-708-5p in MDs, we considered rodents given their extensive use in modelling psychiatric conditions (59). As a first step, we

investigated whether miR-708-5p was expressed in different regions of the rat brain (Fig. 2A). We observed robust expression in regions classically implicated in MDs and cognitive function, such as the amygdala, frontal cortex, and hippocampus (Fig. 2A). Next, we assessed miR-708-5p expression in rat hippocampal primary neurons. Single-molecule fluorescence *in situ* hybridization (sm-FISH) showed that miR-708-5p is expressed in both CamK2a+ excitatory and GAD2+ inhibitory neurons in rat hippocampal cultures, illustrating its widespread neuronal distribution (Fig. 2B and 2C). miR-708-5p expression in rat hippocampal cultures decreased over time during *in vitro* development, indicating a role for miR-708-5p at early stages of neuronal development (Fig. 2D). Motivated by the findings of miR-708-5p elevation in peripheral blood of humans at risk to develop MDs (Fig. 1B-D), we asked whether miR-708-5p was similarly dysregulated in rat genetic and environmental models of MDs. As a genetic model, we chose rats heterozygous for *Cacna1c* (*Cacna1c*$^{+/-}$), a repeatedly validated cross-disorder psychiatric risk gene (60–65). Environmental risk was modelled by juvenile social isolation, a widely recognized model for early life trauma, e.g., childhood maltreatment (66) (Fig. 2E). miR-708-5p was significantly upregulated by social isolation in the hippocampus of juvenile wild-type rats compared to their group-housed counterparts (Fig. 2F), indicating parallels between the early life stress-related modulation of miR-708-5p expression in human peripheral blood and rat brain. Furthermore, *Cacna1c* heterozygosity led to an upregulation of miR-708-5p in the rat hippocampus independent of social housing conditions, suggesting that, like our human PBMC data (Fig. 1C-D), a *genetic* predisposition for MDs is sufficient to induce miR-708-5p expression in the rat brain (Fig. 2F). Our comprehensive analysis across various experimental paradigms revealed that miR-708-5p expression is linked to both environmental stressors and genetic factors associated with MDs in both humans and rodents. Therefore, manipulation of miR-708-5p in the rodent brain represents a viable strategy to study the involvement of miR-708-5p in the development of mood disorder-associated endophenotypes as well as the underlying molecular mechanisms.

miR-708-5p overexpression in the mouse hippocampus recapitulates BD-associated endophenotypes.

We next investigated whether stress-induced upregulation of miR-708-5p in the rodent hippocampus is causally involved in the development of mood disorder-associated behavioral endophenotypes. Towards this end, miR-708-5p was ectopically overexpressed in the mouse hippocampus using stereotactic injection of a recombinant rAAV expressing a miR-708-5p hairpin (hp) under the control of the human synapsin (hSYN) promoter (Fig. S3A). To ensure the functionality of the overexpressing construct, we performed luciferase assay upon transfection of miR-708-5p overexpressing plasmid (hp708-p) together with a luciferase sensor harboring two perfect binding sites for miR-708-5p. Thereby, we detected a significant decrease in luciferase activity upon miR-708-5p overexpression compared to the control (hpCTL-p) (Fig. S3B), demonstrating efficient repression of the reporter gene by the overexpressed miR-708-5p. We went on to perform stereotactic surgeries on seven to eight-week-old mice, which then underwent a four-week recovery period before behavioral assessments were conducted (Fig. 3A). Our approach led to a widespread infection of both the dorsal and ventral hippocampus (Fig. 3B), as well as to a robust miR-708-5p overexpression compared to control infected mice (Fig. 3C; Suppl. Fig. 3C-E). . Male mice overexpressing miR-708-5p in the hippocampus exhibited a significant decrease in immobility during the tail suspension test (TST), indicative of reduced behavioral despair, while this effect was not observed in female mice (Fig. 3D-E). Interestingly, neither male nor female mice with miR-708-5p overexpression showed significant differences in saccharin preference compared to control groups, suggesting no alteration in anhedonia-like behavior (Fig. S3F-G). Furthermore, we observed a strong, although non-significant trend, for elevated anxiety-related compulsive behavior, as assessed by the marble burying test (MBT), in miR-708-5p overexpressing male mice (Fig. 3F). However, results from the elevated plus maze (EPM) did not reveal significant changes in general anxiety levels between the experimental groups (Suppl. Fig 3 H-I). We further evaluated cognitive functions since cognitive impairments are frequently observed in mood disorder patients. Our results from the novel object recognition

(NOR) (Fig. 3G) test revealed that miR-708-5p overexpression led to a significant impairment in object recognition memory after a 24-hour delay specifically in male mice (Fig. 3H; Fig. S4A, B). This impairment was also evident in short-term memory (5 min delay), as miR-708-5p overexpressing mice failed to discriminate between familiar and novel objects after a brief five-minute interval, this time in a sex-independent manner (Fig. 3 I, J; Fig. S4C-F). Passive avoidance, however, was intact in miR-708-5p expressing male mice (Fig. S4G). Locomotor activity, assessed through the OFT remained unchanged, ruling out locomotion as a confounding factor in our behavioral assessments (Fig. S4H-J). Together, our results provide strong evidence that hippocampal overexpression of miR-708-5p leads to distinct mood disorder-associated behaviors. Specifically, reduced behavioral despair, elevated compulsive behavior and impaired recognition memory are consistent with a role for miR-708-5p in the etiology of BD, which aligns with our results from expression analysis in mood disorder patients (Fig. 1). Interestingly, miR-708-5p peripheral expression in human subjects negatively correlated with the score from the D2 attention test (Fig. 3K, S4K and L) in both female and male subjects, further suggesting a role for miR-708-5p in human cognitive processes associated with BD.

miR-708-5p directly targets Neuronatin (Nnat), an ER-resident protein involved in calcium homeostasis.

As a next step, we decided to explore the mechanisms underlying miR-708-5p dependent regulation of BD-associated behavior. miRNAs regulate gene expression through binding to mRNAs, predominantly leading to their degradation or inhibition of translation (15). Therefore, we reasoned that the analysis of the hippocampal transcriptome of miR-708-5p overexpressing mice could inform us about potential miR-708-5p downstream targets mediating behavioral effects. polyA-RNA-sequencing (seq) revealed 118 differentially expressed genes (DEG) (p-value<0.01; FDR<0.001) between the hippocampus of hp-708 and hp-control infected mice (Fig. 4A). Sixteen DEGs were significantly downregulated and contained predicted miR-708-5p binding sites (Fig. 4B), making them strong candidates for direct targets of miR-708-5p. Nnat was of particular interest, since it has been previously identified as a direct target of miR-708-5p (27,33) and its 3'UTR contains a miR-708-5p perfect

binding site (Fig. 4C). The Nnat gene encodes for a small ER-resident protein which acts as an endogenous inhibitor of the SERCA calcium pump, thereby controlling intracellular calcium homeostasis which is disturbed in BD (38). Moreover, within the mouse brain, Nnat is primarily expressed in glutamatergic CA1 and CA3 neurons based on published single cell RNA-seq data (Fig. 4B), consistent with a functional interaction of miR-708-5p and Nnat in neurons. To further validate our RNA-seq data, we measured the levels of Nnat mRNA in the hippocampus of mice upon miR-708-5p overexpression (Fig. 4D) and detected a significant decrease compared to control infected mice (Fig. 4E). So far, our expression analysis on hippocampal tissue did not allow to distinguish between effects occurring in neuronal and non-neuronal cells. Therefore, we further extended our analysis to rat primary hippocampal neuron cultures. Like in the *in vivo* experiments, infection of rat neurons with hp708 resulted in a robust upregulation of miR-708-5p levels (Fig. 4F) and led to significant reductions in Nnat mRNA (Fig. 4G), and protein levels (Fig.4H and I), demonstrating that miR-708-5p represses endogenous Nnat expression in neurons. To prove that the downregulation of Nnat is due to a direct interaction of the miR-708-5p and Nnat mRNA via the predicted miR-708-5p binding site, we performed luciferase reporter gene assay in primary rat hippocampal neurons. Luciferase reporter genes were either fused to the wild type 3'UTR of Nnat (Nnat wt) or to a 3'UTR of Nnat containing several point mutations expected to prevent miR-708-5p binding (Nnat mt). Whereas Nnat wt was efficiently downregulated by co-transfection of hp708-p, Nnat mt was insensitive to miR-708-5p overexpression (Fig. 4J). The results obtained from these assays therefore confirm that miR-708-5p directly suppresses Nnat expression through a 3'UTR interaction. In a complementary approach, we employed a target-directed miRNA degradation (TDMD) construct (sp708-p) to reduce endogenous miR-708-5p levels (Fig. S5A-C). Here, we detected a significant increase in luciferase activity upon transfection with sp708-p compared to control for Nnat wt, but not Nnat mt expressing neurons (Fig. 4K). In summary, our results from RNA-seq, qPCR and luciferase assays establish Nnat as a direct target of miR-708-5p in rodent hippocampal neurons.

Restoring Nnat expression in miR-708-5p overexpressing hippocampal neurons rescues BD-associated behavioral endophenotypes in mice.

Building upon our identification of Nnat as a potential regulatory target of miR-708-5p in the hippocampus, we hypothesized that Nnat downregulation might underlie the observed BD-associated behavioral alterations elicited by miR-708-5p overexpression. To test this hypothesis, we engineered a construct which allows to simultaneously overexpress Nnat and miR-708-5p upon viral infection. This was achieved by inserting the coding sequence of Nnat downstream of the hSYN promoter, coupled with a P2A self-cleaving peptide; this fragment was followed by the EGFP coding sequence and the overexpressing miR-708-5p hairpin. As a control, we utilized a similar construct where the mCherry coding sequence replaced Nnat followed by EGFP and hp708 or EGFP and hpCTL (Fig 5A). rAAV obtained from these constructs was injected into the hippocampus of seven/eight weeks old male mice by stereotaxis, followed by a four-week recovery period before behavioral assessments as described in Fig. 3A. Expression analyses confirmed the upregulation of miR-708-5p and the intended modulation of Nnat levels (Fig. 5B, 5C; Suppl. Fig 6A, and Fig. 5D, Suppl. Fig 6B). Notably, the mCherry-P2A-hp708 construct led to a pronounced upregulation of miR-708-5p (Fig. 5B) and a corresponding decrease in Nnat levels, as opposed to the control and the Nnat-P2A-hp708 conditions, the latter of which restored Nnat expression to wild-type levels (Fig. 5C and Suppl. Fig 6A, B). Behavioral analyses revealed that miR-708-5p overexpression alone impaired object discrimination ability in the NOR test as expected (Fig. 5D, Suppl. Fig. 6F). This was not observed in mice injected with the Nnat-P2A-hp708 construct, which displayed a restoration of exploratory behavior towards the novel object to a similar degree than control injected mice (Fig. 5D, Suppl. Fig. 6F). Furthermore, as expected from our previous results, the total exploration time of the animals was not affected in any of the conditions (Suppl. Fig 6G). Similarly, the TST results indicated reduced behavioral despair in miR-708-5p overexpressing mice, an effect that was normalized upon co-expression of Nnat, again mirroring control group behaviors (Fig. 5E). Furthermore, no significant

differences between experimental groups were observed in locomotor activity in the OFT (Suppl. Fig. 6C-E). Taken together, our results strongly suggest that Nnat is an important downstream target in mediating the effects on BD-associated behavioral endophenotypes caused by miR-708-5p overexpression in the hippocampus.

Discussion

In this study, we found that miR-708-5p is upregulated in healthy human subjects at high risk to develop MDs, in MD patients and in genetic and environmental rat MD models. Furthermore, peripheral miR-708-5p expression was negatively correlated with scores from the D2 attention test. Moreover, miR-708-5p overexpression in the mouse hippocampus led to memory impairments, increased compulsive anxiety and reduced depression-like behavior. Together with the fact that miR-708-5p was nominally associated with BD in a previous GWAS (21), our results strongly implicate this miRNA in the etiology of BD and suggest its potential use as BD biomarker.

miR-708-5p function in BD-associated behaviors

Modelling the complex symptomatology of BD in animal models is challenging and has so far only been partially achieved in mice in the context of miRNA manipulation. For example, the acute manipulation of miR-124 in the PFC of mice led to impaired social behavior and locomotor disturbances upon injection of psychostimulants (67). The hippocampal overexpression of miR-499-5p in *Cacna1c*$^{+/-}$ rats provoked memory impairments, recapitulating the cognitive deficits encountered in BD (22) which include difficulties in attention, memory and executive functions present during the different mood phases and during remission (68). Accordingly, we found that in humans miR-708-5p peripheral expression is negatively correlated with D2 scoring in the attention test (69). Moreover, we found that both female and male mice overexpressing miR-708-5p in the hippocampus showed memory impairments. Furthermore, male, but not female, mice showed significantly decreased immobility in the TST. This test has been historically used to test antidepressant effects on mice but is also employed in mouse models of manic behavior. For example, BD mouse models of mania (Ankyrin-G conditional knockout,

Clock19 deficient mice) show reduced immobility during TST (11) and the FST (10), suggesting that the reduced behavioral despair in our model could reflect a function of miR-708-5p in manic-like behavior. This is further supported by increased (although non-significant) marble burying, indicative of a compulsive response to anxiogenic stimuli. However, in our study, the antidepressant-like behavior was neither accompanied by increased exploratory behavior in the OFT, nor increased risk-taking during EPM testing, both of which are usually observed in mouse models of mania. We consider two possible explanations for this discrepancy. First, contrary to most of the models reported in the literature, our animal model is characterized by an acute and selective overexpression of miR-708-5p in the hippocampus. Therefore, we might expect to observe endophenotypes dependent on the hippocampus (e.g., antidepressant-like behavior, cognition), but not those related to other brain regions, such as the amygdala, prefrontal cortex, or cerebellum (e.g., risk-taking behavior, hyperactivity). Alternatively, the miR-708-5p/Nnat pathway might selectively control specific aspects of manic- and depression-like behavior. To distinguish between these possibilities, it will be important to study the role of miR-708-5p overexpression in other brain areas relevant for BD-associated behaviors in the future.

Role of miR-708-5p in excitatory vs. inhibitory neurons

The balance between excitation and inhibition in neuronal network activity is disrupted in many neuropsychiatric disorders, including MDD (70), BD, and SCZ (71–73). In this regard, inhibitory neuron dysfunction is increasingly considered in MDs. Our approach to overexpress miR-708-5p in the hippocampus using a pan-neuronal promoter (Synapsin-1) does not allow to distinguish the contribution of defects in excitatory and inhibitory neurons to the observed phenotypes. Based on published Ago pull-down and single cell RNA-seq datasets, Nnat is primarily expressed in excitatory neurons (32). In contrast, Nnat was found to be upregulated in parvalbumin-positive (PV+) interneurons of the hippocampus and amygdala in an Angelman Syndrome mouse model (33), as well as in human PV+ interneurons from Lafora Disease patients (74). Hence, the role of miR-708-5p in excitatory and inhibitory neuron populations needs to be further investigated by cell-specific overexpression of miR-708-5p followed by BD-related behavioral characterization.

miR-708-5p regulation by genetic and environmental risk factors

BD has the highest rate of inheritance among psychiatric disorders (up to 70%). However, genetics alone cannot explain the degree at which BD is inherited in families, suggesting that environmental factors need to be considered as well (2,75,76). Childhood maltreatment is the most studied environmental stressor in the context of MDs (3,5,77). Interestingly miR-708-5p was upregulated in the juvenile social isolation rat model, an animal model for childhood maltreatment (78). Consistent with this result, a recent study reported miR-708-5p upregulation in the PFC upon seven days of chronic social defeat in vulnerable rats compared to resilient animals (31). Moreover, miR-708-5p levels are elevated in *Cacna1c*$^{+/-}$ rats, a well-established genetic model of psychiatric disorders (79), even without environmental stressors. Taken together, these results suggest that genetic and environmental risk might impinge on common pathways triggering miR-708-5p expression. Furthermore, studies in the context of ovarian cancer revealed the presence of a glucocorticoid response element upstream of *ODZ4* (29), suggesting that the expression of the host gene and of miR-708-5p might be responsive to glucocorticoids (80). Moreover, studies in the context of ER stress suggest that miR-708-5p expression is induced by CHOP, a transcription factor involved in the Unfolded Protein Response (UPR) upon ER stress (30). Furthermore, metformin-induced upregulation of miR-708-5p elicits Nnat downregulation in prostate cancer, leading to the expression of ER-Stress-mediators. Finally, bisphenol A, an ubiquitous endocrine disruptive chemical, induces miR-708-5p in hypothalamic neurons in a CHOP-dependent manner, accompanied by Nnat downregulation (26). Thus, we speculate that increased ER stress, which has been implicated in BD, is a critical mediator of miR-708-5p upregulation in response to genetic and environmental stress in neurons.

Molecular and cellular mechanisms downstream of the miR-708-5p/Nnat interaction

Dysregulated calcium homeostasis has been previously implicated in the pathophysiology of BD (38). Our results from this and a previous study (22) are consistent with disrupted calcium flux via L-type calcium channels, e.g., due to

Cacna1c mutation, as a major underlying cause. However, ER calcium dynamics emerges as another major player. For example, store operated calcium entry (SOCE) is dysregulated in BD-induced pluripotent stem cells, leading to earlier neuronal differentiation and abnormal neurite outgrowth (81). Furthermore**,** altered expression of the miR-708-5p target Nnat has been associated with defective intracellular and ER calcium levels (33,74,82). Nnat is a small ER membrane protein which acts as an antagonist of the sarco-endoplasmic reticulum calcium ATPase (SERCA) pump, thereby interfering with calcium re-uptake into the ER (35,36). Consistently, it has been reported that miR-708-5p-mediated downregulation of Nnat causes lower basal cytoplasmic calcium levels (33). On the other hand, excessive ER calcium re-uptake could result in ER calcium overload, which in turn leads to calcium leakage to the cytoplasm and mitochondria (83,84), with negative consequences for calcium signaling and cell health, as exemplified in Alzheimer's disease (85,86). Clearly, further studies are warranted on the impact of aberrant miR-708-5p/Nnat signaling on intraneuronal calcium homeostasis in the context of BD.

miR-708-5p as a potential biomarker in BD

Our findings indicate an upregulation of miR-708-5p in PBMCs of females at risk of MDs and in patients with MDD and BD. A previous study reported a downregulated expression of miR-708-5p in leukocytes of women in depressive state compared to women in remission (87). These results are in line with our detected expression difference between female euthymic patients and depressive patients. For male samples, on the other hand, our data suggest a role of miR-708-5p specifically in the manic phase of the disorder, as indicated from the YMRS correlation and the behavioral characterization. Although SCZ and BD were reported to have the highest genetic correlation among psychiatric disorders (77), we found that miR-708-5p expression was unchanged in peripheral samples of patients diagnosed with SCZ. This suggests a rather specific expression pattern of miR-708-5p in the spectrum of MDs. Within MDs, miR-708-5p upregulation was most pronounced in BD. This is impressively illustrated by our ROC curve analysis, which shows that miR-708-5p expression, when combined with miR-499-5p, effectively distinguishes BD patients not only from healthy controls, but also from MDD patients. Although miR-708-5p is significantly upregulated in both male and female BD patient samples, the degree

of increase is higher in males compared to females (8.8-fold vs. 4.23-fold change). Moreover, based on our ROC curve analysis, miR-708-5p expression discriminated male BD patients better from control and MDD compared to female patients. Together, these observations suggest a potential sex-specific role of miR-708-5p in BD, which also aligns with our results from mouse behavior. Sex differences in BD manifest across various aspects, ranging from clinical symptoms to the progression of the disorder. Males typically encounter their first manic episode at a younger age compared to females, who are more likely to experience a depressive episode at the onset of BD (6). In contrast, females experience a higher incidence of depressive episodes and hypomania, leading to a more frequent diagnosis of BD type II (88). Females are also more susceptible to mixed episodes(89), rapid cycling of mood phases (90,91), and show a greater likelihood of attempting suicide (92). Whereas men perform better in working memory tasks, females performed better in verbal learning and memory task recognition (8). In this regard, miRNAs have been previously implicated in SCZ/BD differential regulations of circadian, cholinergic, and neurokine pathways (93).

We propose that miR-708-5p represents a promising candidate for the development of a biomarker that helps to stratify mood disorder patients based on disease entity, specific phases of the disease and sex, which should greatly help with diagnosis and therapy.

Acknowledgements

We greatly acknowledge the technical support in the preparation of primary hippocampal cultures by Cristina Furler, Tatjana Wüst and Dr. Roberto Fiore. We also thank Dr. Brunno Rocha Levone for support in behavioral testing and inputs on the manuscript. We also thank Darren Kelly for support in designing the TDMD construct, and David Colameo and Emanuel Sonder for support in the statistical analysis. RNA sequencing was performed at the Functional Genomics Center Zurich (FGCZ) of the University Zurich and ETH Zurich. The work in the lab of GS was supported by grants from ETH Zurich (ETH-24 18-2 Grant (NeuroSno)) and the Swiss National Science Foundation (SNSF 310030E_179651, 32NE30_189486,

310030_205064/1). This work was further funded by the German Research Foundation (DFG grants FOR2107 KI588/14-1, and KI588/14-2, and KI588/20-1, KI588/22-1 to Tilo Kircher, Marburg, Germany; grant FOR2107 DA1151/5-1, DA1151/5-2, DA1151/9-1, DA1151/10-1, DA1151/11-1 to UD; grant FOR2107 SCHR 1136/3-1 to GS) and the Interdisciplinary Center for Clinical Research (IZKF) of the medical faculty of Münster (grant Dan3/022/22 to UD). Biosamples and corresponding data were sampled, processed and stored in the Marburg Biobank CBBMR.

Author contributions

Carlotta Gilardi: Investigation; writing. Helena Martins: Investigation. Pierre-Luc Germain: Formal analysis. Fridolin Gross: Formal analysis. Alessandra Lo Bianco: Investigation. Silvia Bicker: Investigation; methodology. Ayse Özge Sungur: Investigation. Theresa M. Kisko: Investigation. Rainer K.W. Schwarting: Supervision. Frederike Stein: Data curation; formal analysis. Susanne Meinert: Data curation. Udo Dannlowski: supervision. Tilo Kircher: supervision; project administration. Markus Wöhr: supervision; project administration. Gerhard Schratt: Conceptualization; supervision; writing.

Conflict of Interest

The authors declare that they have no conflict of interest.

Data availability

RNA sequencing data has been deposited to Gene Expression Omnibus (GEO, small RNA-sequencing Fig. 1B-C, accession numbers: GSE261287; RNA-sequencing Fig. 4A, accession numbers: GSE261288).

Bibliography

1. McGuffin P, Rijsdijk F, Andrew M, Sham P, Katz R, Cardno A. The Heritability of Bipolar Affective Disorder and the Genetic Relationship to Unipolar Depression. Arch Gen Psychiatry. 2003 May 1;60(5):497.

2. Craddock N, Sklar P. Genetics of bipolar disorder. The Lancet. 2013 May;381(9878):1654–62.

3. Rodriguez V, Alameda L, Trotta G, Spinazzola E, Marino P, Matheson SL, et al. Environmental Risk Factors in Bipolar Disorder and Psychotic Depression: A Systematic Review and Meta-Analysis of Prospective Studies. Schizophr Bull. 2021 Jul 8;47(4):959–74.

4. Nemeroff CB. Paradise Lost: The Neurobiological and Clinical Consequences of Child Abuse and Neglect. Neuron. 2016 Mar;89(5):892–909.

5. Aas M, Bellivier F, Bettella F, Henry C, Gard S, Kahn J-P, et al. Childhood maltreatment and polygenic risk in bipolar disorders. Bipolar Disord. 2020;22(2):174–81.

6. Kennedy N, Everitt B, Boydell J, Os JV, Jones PB, Murray RM. Incidence and distribution of first-episode mania by age: results from a 35-year study. Psychol Med. 2005 Jun;35(6):855–63.

7. Zhang L, Swaab DF. Sex differences in bipolar disorder: The dorsolateral prefrontal cortex as an etiopathogenic region. Front Neuroendocrinol. 2024 Jan 1;72:101115.

8. Arnold LM. Gender differences in bipolar disorder. Psychiatr Clin North Am. 2003 Sep 1;26(3):595–620.

9. Li X, Chen B, Zhang D, Wang S, Feng Y, Wu X, et al. A novel murine model of mania. Mol Psychiatry. 2023 Jul;28(7):3044–54.

10. Roybal K, Theobold D, Graham A, DiNieri JA, Russo SJ, Krishnan V, et al. Mania-like behavior induced by disruption of CLOCK. Proc Natl Acad Sci. 2007 Apr 10;104(15):6406–11.

11. Zhu S, Cordner ZA, Xiong J, Chiu C-T, Artola A, Zuo Y, et al. Genetic disruption of ankyrin-G in adult mouse forebrain causes cortical synapse alteration and behavior reminiscent of bipolar disorder. Proc Natl Acad Sci. 2017 Sep 26;114(39):10479–84.

12. Kozikowski AP, Gaisina IN, Yuan H, Petukhov PA, Blond SY, Fedolak A, et al. Structure-Based Design Leads to the Identification of Lithium Mimetics That Block Mania-like Effects in Rodents. Possible New GSK-3β Therapies for Bipolar Disorders. J Am Chem Soc. 2007 Jul 1;129(26):8328–32.

13. Dao DT, Mahon PB, Cai X, Kovacsics CE, Blackwell RA, Arad M, et al. Mood Disorder Susceptibility Gene CACNA1C Modifies Mood-Related Behaviors in Mice and Interacts with Sex to Influence Behavior in Mice and Diagnosis in Humans. Biol Psychiatry. 2010 Nov 1;68(9):801–10.

14. Martins HC, Schratt G. MicroRNA-dependent control of neuroplasticity in affective disorders. Transl Psychiatry. 2021 May 3;11(1):263.

15. Bartel DP. Metazoan MicroRNAs. Cell. 2018 Mar;173(1):20–51.

16. Schratt G. microRNAs at the synapse. Nat Rev Neurosci. 2009 Dec;10(12):842–9.

17. Emde A, Hornstein E. miRNAs at the interface of cellular stress and disease. EMBO J. 2014 Jul;33(13):1428–37.

18. Moreau MP, Bruse SE, David-Rus R, Buyske S, Brzustowicz LM. Altered microRNA expression profiles in post-mortem brain samples from individuals with schizophrenia and bipolar disorder. Biol Psychiatry. 2011 Jan 15;69(2):188–93.

19. Zhang Z, Convertini P, Shen M, Xu X, Lemoine F, de la Grange P, et al. Valproic Acid Causes Proteasomal Degradation of DICER and Influences miRNA Expression. Pfeffer S, editor. PLoS ONE. 2013 Dec 17;8(12):e82895.

20. Coradduzza D, Garroni G, Congiargiu A, Balzano F, Cruciani S, Sedda S, et al. MicroRNAs, Stem Cells in Bipolar Disorder, and Lithium Therapeutic Approach. Int J Mol Sci. 2022 Jan;23(18):10489.

21. Forstner AJ, Hofmann A, Maaser A, Sumer S, Khudayberdiev S, Mühleisen TW, et al. Genome-wide analysis implicates microRNAs and their target genes in the development of bipolar disorder. Transl Psychiatry. 2015 Nov 10;5(11):e678–e678.

22. Martins HC, Gilardi C, Sungur AÖ, Winterer J, Pelzl MA, Bicker S, et al. Bipolar-associated miR-499-5p controls neuroplasticity by downregulating the Cav1.2 subunit CACNB2. EMBO Rep. 2022 Oct 6;23(10):e54420.

23. He S, Liu X, Jiang K, Peng D, Hong W, Fang Y, et al. Alterations of microRNA-124 expression in peripheral blood mononuclear cells in pre- and post-treatment patients with major depressive disorder. J Psychiatr Res. 2016 Jul;78:65–71.

24. Liu S, Zhang F, Shugart YY, Yang L, Li X, Liu Z, et al. The early growth response protein 1-miR-30a-5p-neurogenic differentiation factor 1 axis as a novel biomarker for schizophrenia diagnosis and treatment monitoring. Transl Psychiatry. 2017 Jan 10;7(1):e998–e998.

25. Psychiatric GWAS Consortium Bipolar Disorder Working Group, Sklar P, Ripke S, Scott LJ, Andreassen OA, Cichon S, et al. Large-scale genome-wide association analysis of bipolar disorder identifies a new susceptibility locus near ODZ4. Nat Genet. 2011 Oct;43(10):977–83.

26. McIlwraith EK, Lieu CV, Belsham DD. Bisphenol A induces miR-708-5p through an ER stress-mediated mechanism altering neuronatin and neuropeptide Y expression in hypothalamic neuronal models. Mol Cell Endocrinol. 2022 Jan 1;539:111480.

27. Yang J, Wei J, Wu Y, Wang Z, Guo Y, Lee P, et al. Metformin induces ER stress-dependent apoptosis through miR-708-5p/NNAT pathway in prostate cancer. Oncogenesis. 2015 Jun 15;4(6):e158–e158.

28. Rodríguez-Comas J, Moreno-Asso A, Moreno-Vedia J, Martín M, Castaño C, Marzà-Florensa A, et al. Stress-Induced MicroRNA-708 Impairs β-Cell Function and Growth. Diabetes. 2017 Dec 1;66(12):3029–40.

29. Lin K-T, Yeh Y-M, Chuang C-M, Yang SY, Chang J-W, Sun S-P, et al. Glucocorticoids mediate induction of microRNA-708 to suppress ovarian cancer metastasis through targeting Rap1B. Nat Commun. 2015 Jan 8;6(1):5917.

30. Behrman S, Acosta-Alvear D, Walter P. A CHOP-regulated microRNA controls rhodopsin expression. J Cell Biol. 2011 Mar 21;192(6):919–27.

31. Chen RJ, Kelly G, Sengupta A, Heydendael W, Nicholas B, Beltrami S, et al. MicroRNAs as biomarkers of resilience or vulnerability to stress. Neuroscience. 2015 Oct 1;305:36–48.

32. Oyang EL, Davidson BC, Lee W, Poon MM. Functional Characterization of the Dendritically Localized mRNA Neuronatin in Hippocampal Neurons. Amédée T, editor. PLoS ONE. 2011 Sep 14;6(9):e24879.

33. Vatsa N, Kumar V, Singh BK, Kumar SS, Sharma A, Jana NR. Down-Regulation of miRNA-708 Promotes Aberrant Calcium Signaling by Targeting Neuronatin in a Mouse Model of Angelman Syndrome. Front Mol Neurosci. 2019 Feb 13;12:35.

34. Ryu S, McDonnell K, Choi H, Gao D, Hahn M, Joshi N, et al. Suppression of miRNA-708 by Polycomb Group Promotes Metastases by Calcium-Induced Cell Migration. Cancer Cell. 2013 Jan;23(1):63–76.

35. Braun JL, Teng ACT, Geromella MS, Ryan CR, Fenech RK, MacPherson REK, et al. Neuronatin promotes SERCA uncoupling and its expression is altered in skeletal muscles of high-fat diet-fed mice. FEBS Lett. 2021;595(22):2756–67.

36. Lin H-H, Bell E, Uwanogho D, Perfect LW, Noristani H, Bates TJD, et al. Neuronatin Promotes Neural Lineage in ESCs via Ca2+ Signaling. Stem Cells. 2010 Nov 1;28(11):1950–60.

37. Viswanath B, Jose SP, Squassina A, Thirthalli J, Purushottam M, Mukherjee O, et al. Cellular models to study bipolar disorder: A systematic review. J Affect Disord. 2015 Sep 15;184:36–50.

38. Harrison PJ, Hall N, Mould A, Al-Juffali N, Tunbridge EM. Cellular calcium in bipolar disorder: systematic review and meta-analysis. Mol Psychiatry. 2021 Aug;26(8):4106–16.

39. Kircher T, Wöhr M, Nenadic I, Schwarting R, Schratt G, Alferink J, et al. Neurobiology of the major psychoses: a translational perspective on brain structure and function—the FOR2107 consortium. Eur Arch Psychiatry Clin Neurosci. 2019 Dec 1;269(8):949–62.

40. Wittchen H-U, Wunderlich U, Gruschwitz S, Zaudig M. SKID I. Strukturiertes Klinisches Interview für DSM-IV. Achse I: Psychische Störungen. Interviewheft und Beurteilungsheft. Eine deutschsprachige, erweiterte Bearb. d. amerikanischen Originalversion des SKID I. 1997;

41. World Health Organization, editor. The ICD-10 classification of mental and behavioural disorders: clinical descriptions and diagnostic guidelines. Geneva: World Health Organization; 1992. 362 p.

42. Walker EA, Gelfand A, Katon WJ, Koss MP, Von Korff M, Bernstein D, et al. Adult health status of women with histories of childhood abuse and neglect. Am J Med. 1999 Oct 1;107(4):332–9.

43. Brickenkamp R. Der Aufmerksamkeits-Belastungstest d2. Hogrefe, Göttingen; 2002.

44. Chen C-J, Servant N, Toedling J, Sarazin A, Marchais A, Duvernois-Berthet E, et al. ncPRO-seq: a tool for annotation and profiling of ncRNAs in sRNA-seq data. Bioinformatics. 2012 Dec 1;28(23):3147–9.

45. Ritchie ME, Phipson B, Wu D, Hu Y, Law CW, Shi W, et al. limma powers differential expression analyses for RNA-sequencing and microarray studies. Nucleic Acids Res. 2015 Apr 20;43(7):e47.

46. Christensen M. Recombinant adeno-associated virus-mediated microRNA delivery into the postnatal mouse brain reveals a role for miR-134 in dendritogenesis in vivo. Front Neural Circuits. 2010;

47. Daswani R, Gilardi C, Soutschek M, Nanda P, Weiss K, Bicker S, et al. MicroRNA-138 controls hippocampal interneuron function and short-term memory in mice. Huguenard JR, editor. eLife. 2022 Mar 15;11:e74056.

48. Levone BR, Moloney GM, Cryan JF, O'Leary OF. Specific sub-regions along the longitudinal axis of the hippocampus mediate antidepressant-like behavioral effects. Neurobiol Stress. 2021 May;14:100331.

49. Can A, Dao DT, Terrillion CE, Piantadosi SC, Bhat S, Gould TD. The Tail Suspension Test. J Vis Exp JoVE. 2012 Jan 28;(59):3769.

50. Dobin A, Davis CA, Schlesinger F, Drenkow J, Zaleski C, Jha S, et al. STAR: ultrafast universal RNA-seq aligner. Bioinformatics. 2013 Jan 1;29(1):15–21.

51. Liao Y, Smyth GK, Shi W. featureCounts: an efficient general purpose program for assigning sequence reads to genomic features. Bioinformatics. 2014 Apr 1;30(7):923–30.

52. Robinson MD, McCarthy DJ, Smyth GK. edgeR: a Bioconductor package for differential expression analysis of digital gene expression data. Bioinformatics. 2010 Jan 1;26(1):139–40.

53. Leek JT, Johnson WE, Parker HS, Jaffe AE, Storey JD. The sva package for removing batch effects and other unwanted variation in high-throughput experiments. Bioinformatics. 2012 Mar 15;28(6):882–3.

54. Agarwal V, Bell GW, Nam J-W, Bartel DP. Predicting effective microRNA target sites in mammalian mRNAs. Izaurralde E, editor. eLife. 2015 Aug 12;4:e05005.

55. Craddock N, O'Donovan MC, Owen MJ. The genetics of schizophrenia and bipolar disorder: dissecting psychosis. J Med Genet. 2005 Mar 1;42(3):193–204.

56. Vieta E, Salagre E, Grande I, Carvalho AF, Fernandes BS, Berk M, et al. Early Intervention in Bipolar Disorder. Am J Psychiatry. 2018 May;175(5):411–26.

57. Nierenberg AA, Agustini B, Köhler-Forsberg O, Cusin C, Katz D, Sylvia LG, et al. Diagnosis and Treatment of Bipolar Disorder: A Review. JAMA. 2023 Oct 10;330(14):1370.

58. Cao R, López-de-Ullibarri I. ROC Curves for the Statistical Analysis of Microarray Data. In: Bolón-Canedo V, Alonso-Betanzos A, editors. Microarray Bioinformatics. New York, NY: Springer New York; 2019. p. 245–53. (Methods in Molecular Biology; vol. 1986).

59. Yao Z, van Velthoven CTJ, Nguyen TN, Goldy J, Sedeno-Cortes AE, Baftizadeh F, et al. A taxonomy of transcriptomic cell types across the isocortex and hippocampal formation. Cell. 2021 Jun;184(12):3222-3241.e26.

60. Bhat S, Dao DT, Terrillion CE, Arad M, Smith RJ, Soldatov NM, et al. CACNA1C (Cav1.2) in the pathophysiology of psychiatric disease. Prog Neurobiol. 2012 Oct 1;99(1):1–14.

61. Harrison PJ, Husain SM, Lee H, Los Angeles AD, Colbourne L, Mould A, et al. CACNA1C (CaV1.2) and other L-type calcium channels in the pathophysiology and treatment of psychiatric disorders: Advances from functional genomics and pharmacoepidemiology. Neuropharmacology. 2022 Dec 1;220:109262.

62. Ferreira MAR, O'Donovan MC, Meng YA, Jones IR, Ruderfer DM, Jones L, et al. Collaborative genome-wide association analysis supports a role for ANK3 and CACNA1C in bipolar disorder. Nat Genet. 2008 Sep;40(9):1056–8.

63. Dedic N, Pöhlmann ML, Richter JS, Mehta D, Czamara D, Metzger MW, et al. Cross-disorder risk gene CACNA1C differentially modulates susceptibility to

psychiatric disorders during development and adulthood. Mol Psychiatry. 2018;23(3):533–43.

64. Dao DT, Mahon PB, Cai X, Kovacsics CE, Blackwell RA, Arad M, et al. Mood Disorder Susceptibility Gene CACNA1C Modifies Mood-Related Behaviors in Mice and Interacts with Sex to Influence Behavior in Mice and Diagnosis in Humans. Biol Psychiatry. 2010 Nov;68(9):801–10.

65. Bavley CC, Fischer DK, Rizzo BK, Rajadhyaksha AM. Cav1.2 channels mediate persistent chronic stress-induced behavioral deficits that are associated with prefrontal cortex activation of the p25/Cdk5-glucocorticoid receptor pathway. Neurobiol Stress. 2017 Dec 1;7:27–37.

66. Seffer D, Rippberger H, Schwarting RKW, Wöhr M. Pro-social 50-kHz ultrasonic communication in rats: post-weaning but not post-adolescent social isolation leads to social impairments—phenotypic rescue by re-socialization. Front Behav Neurosci. 2015 May 1;9.

67. Namkung H, Yukitake H, Fukudome D, Lee BJ, Tian M, Ursini G, et al. The miR-124-AMPAR pathway connects polygenic risks with behavioral changes shared between schizophrenia and bipolar disorder. Neuron. 2023 Jan 18;111(2):220-235.e9.

68. Huang Y, Zhang Z, Lin S, Zhou H, Xu G. Cognitive Impairment Mechanism in Patients with Bipolar Disorder. Neuropsychiatr Dis Treat. 2023 Feb;Volume 19:361–6.

69. Camelo EVM, Mograbi D, de Assis da Silva R, Bifano J, Wainstok M, Silveira LAS, et al. Performance of Bipolar Disorder Patients in Attention Testing: Comparison with Normal Controls and Among Manic, Depressive, and Euthymic Phases. Psychiatr Q. 2017 Mar 1;88(1):55–63.

70. Fee C, Banasr M, Sibille E. Somatostatin-Positive Gamma-Aminobutyric Acid Interneuron Deficits in Depression: Cortical Microcircuit and Therapeutic Perspectives. Biol Psychiatry. 2017 Oct;82(8):549–59.

71. Lewis DA, Sweet RA. Schizophrenia from a neural circuitry perspective: advancing toward rational pharmacological therapies. J Clin Invest. 2009 Apr 1;119(4):706–16.

72. Sakai T, Oshima A, Nozaki Y, Ida I, Haga C, Akiyama H, et al. Changes in density of calcium-binding-protein-immunoreactive GABAergic neurons in prefrontal cortex in schizophrenia and bipolar disorder. Neuropathology. 2008;28(2):143–50.

73. Fung SJ, Fillman SG, Webster MJ, Shannon Weickert C. Schizophrenia and bipolar disorder show both common and distinct changes in cortical interneuron markers. Schizophr Res. 2014 May 1;155(1):26–30.

74. Sharma J, Mukherjee D, Rao SNR, Iyengar S, Shankar SK, Satishchandra P, et al. Neuronatin-mediated Aberrant Calcium Signaling and Endoplasmic Reticulum

Stress Underlie Neuropathology in Lafora Disease. J Biol Chem. 2013 Mar;288(13):9482–90.

75. Burmeister M, McInnis MG, Zöllner S. Psychiatric genetics: progress amid controversy. Nat Rev Genet. 2008 Jul;9(7):527–40.

76. Craddock N, Sklar P. Genetics of bipolar disorder: successful start to a long journey. Trends Genet. 2009 Feb;25(2):99–105.

77. Robinson N, Bergen SE. Environmental Risk Factors for Schizophrenia and Bipolar Disorder and Their Relationship to Genetic Risk: Current Knowledge and Future Directions. Front Genet. 2021;12.

78. Toda T, Parylak S, Linker SB, Gage FH. The role of adult hippocampal neurogenesis in brain health and disease. Mol Psychiatry. 2019 Jan;24(1):67–87.

79. Wöhr M, Kisko TM, Schwarting RKW. Social Behavior and Ultrasonic Vocalizations in a Genetic Rat Model Haploinsufficient for the Cross-Disorder Risk Gene Cacna1c. Brain Sci. 2021 Jun;11(6):724.

80. Srinivasan S, Shariff M, Bartlett S. The Role of the Glucocorticoids in Developing Resilience to Stress and Addiction. Front Psychiatry. 2013;4.

81. Hewitt T, Alural B, Tilak M, Wang J, Becke N, Chartley E, et al. Bipolar disorder-iPSC derived neural progenitor cells exhibit dysregulation of store-operated Ca2+ entry and accelerated differentiation. Mol Psychiatry. 2023 Jul 4;1–14.

82. Zou H-Y, Guo L, Zhang B, Chen S, Wu X-R, Liu X-D, et al. Aberrant miR-339-5p/neuronatin signaling causes prodromal neuronal calcium dyshomeostasis in mutant presenilin mice. J Clin Invest. 2022 Apr 15;132(8):e149160.

83. Wang Q-C, Zheng Q, Tan H, Zhang B, Li X, Yang Y, et al. TMCO1 Is an ER Ca 2+ Load-Activated Ca 2+ Channel. Cell. 2016 Jun;165(6):1454–66.

84. Daverkausen-Fischer L, Pröls F. Regulation of calcium homeostasis and flux between the endoplasmic reticulum and the cytosol. J Biol Chem. 2022 Jul 1;298(7):102061.

85. Tu H, Nelson O, Bezprozvanny A, Wang Z, Lee S-F, Hao Y-H, et al. Presenilins Form ER Ca2+ Leak Channels, a Function Disrupted by Familial Alzheimer's Disease-Linked Mutations. Cell. 2006 Sep 8;126(5):981–93.

86. Bezprozvanny I, Mattson MP. Neuronal calcium mishandling and the pathogenesis of Alzheimer's disease. Trends Neurosci. 2008 Sep 1;31(9):454–63.

87. Banach E, Dmitrzak-Weglarz M, Pawlak J, Kapelski P, Szczepankiewicz A, Rajewska-Rager A, et al. Dysregulation of miR-499, miR-708 and miR-1908 during a depression episode in bipolar disorders. Neurosci Lett. 2017 Jul;654:117–9.

88. Diflorio A, Jones I. Is sex important? Gender differences in bipolar disorder. Int Rev Psychiatry. 2010 Oct 1;22(5):437–52.

89. Arnold LM, McElroy SL, Keck PE. The role of gender in mixed mania. Compr Psychiatry. 2000;41(2):83–7.

90. Slyepchenko A, Frey BN, Lafer B, Nierenberg AA, Sachs GS, Dias RS. Increased illness burden in women with comorbid bipolar and premenstrual dysphoric disorder: data from 1 099 women from STEP-BD study. Acta Psychiatr Scand. 2017 Nov;136(5):473–82.

91. Tondo L, Baldessarini RJ. Rapid cycling in women and men with bipolar manic-depressive disorders. Am J Psychiatry. 1998 Oct;155(10):1434–6.

92. Clements C, Morriss R, Jones S, Peters S, Roberts C, Kapur N. Suicide in bipolar disorder in a national English sample, 1996-2009: frequency, trends and characteristics. Psychol Med. 2013 Dec;43(12):2593–602.

93. Lobentanzer S, Hanin G, Klein J, Soreq H. Integrative Transcriptomics Reveals Sexually Dimorphic Control of the Cholinergic/Neurokine Interface in Schizophrenia and Bipolar Disorder. Cell Rep. 2019 Oct 15;29(3):764-777.e5.

Figure legends

Fig. 1 miR-708-5p is upregulated in the peripheral blood of human subjects at risk for or diagnosed with MDs.

A. Schematic representation of the workflow to obtain PBMCs samples from the FOR2107 cohort (see also materials and methods) (39). Subjects underwent psychiatric and cognitive evaluation. After the data was collected, blood was withdrawn and PBMCs prepared followed by RNA extraction and downstream gene expression analysis. Samples were collected from psychiatrically healthy female subjects (CTL), or psychiatrically healthy female subjects with genetic predisposition for mood disorder (GR) or that suffered from childhood maltreatment (ER) (Vulnerability samples). Samples were also collected from male and female patients that were diagnosed with Major Depressive Disorder (MDD) or Bipolar Disorder (BD) (mood disorder samples).

B. and C. Volcano plot depicting miRNAs differentially expressed based on small RNA sequencing performed with RNA isolated from PBMCs of control subjects (CTL; n=18), healthy subjects who suffered childhood maltreatment (Environmental risk, ER; n=18), or healthy subjects with a genetic risk (GR; n=14). CTL vs ER (B) or GR (C): miRNAs that are significantly downregulated (logFC<0.5, p-value<0.05) are marked in red; miRNAs that are significantly upregulated (logFC>0.5, p-value<0.05) in blue. Each Volcano Plot is accompanied by a table showing the top 15 differentially expressed genes ordered from smallest to largest p-value. miRNAs overlapping between (B) and (C) are highlighted.

D. miR-708-5p qPCR analysis of total RNA isolated from PBMCs of control subjects (CTL=18), or healthy subjects who suffered childhood Maltreatment (Environmental risk, ER= 16), or healthy subjects with a genetic risk (GR=18). One-way ANOVA with Holm-Sidak's multiple comparisons test, HC vs ER, **, P=0.0064; HC vs GR, ***, P=0.0006; ER vs GR, ns. Data are presented as violin plots with median, quartiles and data points.

E. miR-708-5p qPCR analysis of total RNA isolated from PBMCs of female patients diagnosed with BD or MDD (control: CTL= 26; MDD= 18; BD= 26). Wilcoxon rank-sum test after correction for age and antidepressant treatment; linear model of the form -DeltaCq ~ Group + Age + Antidepressant treatment. Females: CTL vs MDD, *, p<0.05; CTL vs BD, ****, p<0.0005.

F. miR-708-5p qPCR analysis of total RNA isolated from PBMCs of male patients diagnosed with BD or MDD (control: CTL=31; MDD=24; BD= 37. Wilcoxon rank-sum test after correction for age and antidepressant treatment; linear model of the form -DeltaCq ~ Group + Age + Antidepressant treatment. CTL vs MDD, p=0.0549; CTL vs BD, ****, p<0.0005). Data are presented as violin plots with median, quartiles and data points.

G. Correlation plot between the peripheral levels of miR-708-5p in male BD samples (n=37) and Young Mania Rating Scale. Spearman correlation coefficient with two-tailed analysis. Data are presented as XY tables.

H. Correlation plot between the peripheral levels of miR-708-5p in female samples (n=26) and Young Mania Rating Scale. Spearman correlation coefficient with two-tailed analysis. Data are presented as XY tables.

I. ROC curve of combined miR-708-5p and miR-499-5p expression in female (left) and male (right) subjects to discriminate BD vs controls and MDD samples. The indicated thresholds are the closest point to the optimal (i.e. top-left).

Figure 2. miR-708-5p is expressed in rat hippocampal neurons and upregulated in the hippocampus of rat models of environmental or genetic risk for MDs.

A. miR-708-5p qPCR analysis using total RNA isolated from different areas of the adult female rat brain. Data are represented as bar graphs, mean ± SD (n=3 animals).

B. Single-molecule fluorescence *in situ* hybridization (smFISH) performed in rat hippocampal neurons at 7 days *in vitro* (DIV7) using probes directed against miR-708-5p (red channel) and CamK2a (green channel) to identify excitatory neurons. Scale bar: 20μm.

C. smFISH performed in rat hippocampal neurons at DIV7 using probes against miR-708-5p (red channel) and Gad2 (green channel) to identify inhibitory neurons. Scale bar: 20μm.

D. Relative expression of miR-708-5p in primary rat hippocampal neurons at different DIV (n = 3 independent experiments) normalized to U6 snRNA. Data are represented on XY graph as mean ±SD.

E. Schematic representation of the juvenile social isolation experiment, n=9 for each experimental group; PND: postnatal day.

F. miR-708-5p qPCR analysis of total RNA isolated from hippocampi of Wild type (WT) or *Cacna1c*$^{+/-}$ male juvenile rats that were either group-housed or socially isolated for four weeks (n=9 in each group). WT group-housed vs WT Isolated: *, p=0.0265; WT group-housed vs *Cacna1c*$^{+/-}$: **, p=0.0026; linear mixed model, -DeltaCq ~ Genotype * Housing + (1| Cohort), followed by post hoc pairwise comparison with emmeans package (pairwise ~ Genotype * Housing); ns: non-significant. Data are represented as box plot with whiskers and data points (+: mean, line: median; whiskers: minimum and maximum values).

Figure 3. miR-708-5p overexpression in the mouse hippocampus recapitulates BD-associated endophenotypes.

A. Schematic timeline of the acute rAAV stereotactic injection of control (hpCTL) or miR-708-OE (hp708) virus into the dorsal and ventral hippocampus of mice at PNW 7/8, followed by behavioral testing at PNW 11/12.

B. Coronal brain section of mouse brains displaying intense GFP expression upon infection with hp708 virus in the dorsal (up) and ventral (down) hippocampus. Scale bar: 2000 µm.

C. miR-708-5p qPCR analysis of total RNA isolated from hippocampus of mice that underwent behavioral testing. upon miR-708-5p overexpression. hpCTL n=39, hp708 n=39. Unpaired t-Test, ****, p<0.00001. Data are represented as box plot with whiskers and data points (+: mean, line: median; whiskers: minimum and maximum values).

D. Tail Suspension Test. Time (s) male mice injected with the indicated rAAV (hpCTL or hp708, n=15 each) spent immobile. Data are represented as box plot with whiskers and data points (+: mean, line: median; whiskers: minimum and maximum values). Unpaired t-test, ****, p<0.0001.

E. Tail Suspension Test. Time (s) female mice injected with the indicated rAAV (hpCTL n= 12, or hp708, n=11) spent immobile. Data are represented as box plot with whiskers and data points (+: mean, line: median; whiskers: minimum and maximum values). Unpaired t-test, ns.

F. Marble Burying test. Number of marbles male mice injected with the indicated rAAV (hpCTL n= 11, or hp708, n=12) buried in 30 minutes. Data are represented as box plot with whiskers and data points (+: mean, line: median; whiskers: minimum and maximum values). Unpaired t-test, ns, p=0.0524.

G. Schematic representation of the Novel Object Recognition (NOR) Test.mice are exposed to two familiar objects during the familiarization phase. After five

minutes, they are returned to the home cage for either 24 hours or 5 minutes. They are then exposed to a novel and a familiar object during the test phase.

H. Novel object recognition Test with 24 hours break in between familiarization and novelty testing. Time (s) male mice injected with the indicated rAAV (hpCTL n= 10, or hp708, n=12) explored either the familiar (F) or novel (N) object. Data are represented as box plot with whiskers and data points (+: mean, line: median; whiskers: minimum and maximum values). Two-way RM ANOVA: Novelty x Group, ***, p=0.0004; Novelty, ****, p<0.0001; Group, ns, p=0.8830. Šídák's post hoc test, F vs N: hpCTL, ****, p<0.0001; hp708, ns, p=0.6735.

I. Novel object recognition Test with 5 minutes break in between familiarization and novelty testing. Time (s) male mice injected with the indicated rAAV (hpCTL or hp708, n=15 each) explored either the familiar (F) or novel (N) object. Data are represented as box plot with whiskers and data points (+: mean, line: median; whiskers: minimum and maximum values). Two-way RM ANOVA: Novelty x Group, ****, p<0.0001; Novelty, ****, p<0.0001; Group, ns, p=0.8207. Šídák's post hoc test, F vs N: hpCTL, ****, p<0.0001; hp708, ns, p=0.6975.

J. Novel object recognition Test with 5 minutes break in between familiarization and novelty testing. Time (s) female mice injected with the indicated rAAV (hpCTL n= 12, or hp708, n=11) explored either the familiar (F) or novel (N) object. Data are represented as box plot with whiskers and data points (+: mean, line: median; whiskers: minimum and maximum values). Two-way RM ANOVA: Novelty x Group, *, p<0.0130; Novelty, ***, p=0.0001; Group, ns, p=0.8143. Šídák's post hoc test, F vs N: hpCTL, ****, p<0.0001; hp708, ns, p=0.3127.

K. Pearson correlation plot of miR708 peripheral levels and attention (d2 test) in all human participants (female + male, CTL + MDD + BD, n=162), **, p=.005, r=-.223.

Figure 4. miR-708-5p directly targets Nnat, an ER-resident protein involved in calcium homeostasis.

A. Volcano plot depicting differential gene expression in the hippocampus between hp708 and hpCTL injected mice based on polyA-RNA sequencing.

B. Heatmap displaying miR-708-5p predicted targets which are significantly downregulated from (A), as well as their expression in different cell types based on single-cell RNA-seq data (Allen 10X+smartSeq taxonomy)(59). The red rectangle highlights Nnat.

C. Nucleotide base pairing depicting the perfect binding of miR-708-5p with the mouse Nnat 3'-UTR.

D. miR-708-5p qPCR analysis of total RNA isolated from mouse hippocampi upon miR-708-5p overexpression. hpCTL n=17, hp708 n=17. Unpaired t-Test, ****, p<0.00001. Data are represented as box plot with whiskers and data points (+: mean, line: median; whiskers: minimum and maximum values).

E. Neuronatin qPCR analysis of total RNA isolated from mouse hippocampi upon miR-708-5p overexpression. hpCTL n=13, hp708 n=15. Unpaired t-Test, ****, p=0.0269. Data are represented as box plot with whiskers and data points (+: mean, line: median; whiskers: minimum and maximum values).

F. miR-708-5p qPCR analysis of total RNA isolated from rat primary hippocampal neurons at DIV20 infected with hpCTL or hp708 for miR-708-5p overexpression. hpCTL n=4, hp708 n=5. Unpaired t-Test, *, p=0.0317. Data are represented as box plot with whiskers and data points (+: mean, line: median; whiskers: minimum and maximum values).

G. Neuronatin qPCR analysis of total RNA isolated from rat primary hippocampal neurons at DIV20 infected with hpCTL or hp708 for miR-708-5p overexpression. hpCTL n=4, hp708 n=5. Unpaired t-Test, *, p=0.0159. Data are represented as box plot with whiskers and data points (+: mean, line: median; whiskers: minimum and maximum values).

H. Representative Western blot image of Nnat (lower panel) and Tubulin (upper panel) protein expression levels in hippocampal neurons (DIV20) that were infected with hpCTL or hp708 for miR-708-5p overexpression on DIV2. Tubulin was used as a loading control.

I. Quantification of the relative intensity of Nnat protein levels in hippocampal neurons (DIV20) that were infected with hpCTL or hp708 for miR-708-5p overexpression on DIV2 based on (G). Tubulin was used as normalizer. Ratio-paired t-test, **, p=0.0042. n=4 per experimental group. Data are represented as box plot with whiskers and data points (+: mean, line: median; whiskers: minimum and maximum values).

J. Relative luciferase activity of rat hippocampal neurons transfected with the indicated plasmid (Control: hpCTL-p; overexpressing miR-708-5p: hp708-p) and expressing either Nnat wild-type (wt) or miR-708-5p binding site mutant (mt) reporter genes. Data are represented as scattered dot plots with bar, mean±SD (n=4 independent experiments; Two-way ANOVA: main effect of the hairpin *p=0.0245, of the Nnat luciferase reporter **p=0.0050, and of the hairpin by Nnat luciferase reporter interaction p<0.0374. Sidak's post hoc test: **p=0.0092).

K. Relative luciferase activity of rat hippocampal neurons transfected with the indicated plasmid (Control: spCTL-p; knocking-down miR-708-5p: sp708-p) and expressing either Nnat wt or mt reporter genes. Data are represented as scattered dot plots with bar, mean±SD (n=4 independent experiments; Two-way ANOVA: main effect of the hairpin *p=0.0211, no main effect of the Nnat luciferase reporter, or of the hairpin by Nnat luciferase reporter interaction. Sidak's post hoc test: *p=0.0287).

Figure 5. Restoring Nnat expression in miR-708-5p overexpressing hippocampal neurons rescues BD-associated behaviors in mice.

A. Schematic representation of the three rAAV constructs used in the rescue experiment.

B. miR-708-5p qPCR analysis of total RNA isolated from the hippocampus of male mice injected with mCherry-P2A-hpCTL (n=9), mCherry-P2A-hp708 (n12), or Nnat-P2A-hp708 (n=12) viruses. One-way ANOVA, Post hoc Tukey's Test: mCherry-P2A-hpCTL vs mCherry-P2A-hp708: ****, p<0.0001, mCherry-P2A-hpCTL vs Nnat-P2A-hp708: ***, p<0.0001, mCherry-P2A-hp708 vs Nnat-P2A-hp708: ns, p=0.1225. Data are represented as box plot with whiskers and data points (+: mean, line: median; whiskers: minimum and maximum values).

C. Neuronatin qPCR analysis of total RNA isolated from the hippocampus of male mice injected with mCherry-P2A-hpCTL (n=9), mCherry-P2A-hp708 (n12), or Nnat-P2A-hp708 (n=12) viruses. One-way ANOVA, Post hoc Tukey's Test: mCherry-P2A-hpCTL vs mCherry-P2A-hp708: ***, p=0.0003, mCherry-P2A-hpCTL vs Nnat-P2A-hp708: ns, p=0.7379, mCherry-P2A-hp708 vs Nnat-P2A-hp708: ****, p<0.0001. Data are represented as box plot with whiskers and data points (+: mean, line: median; whiskers: minimum and maximum values).

D. Novel object recognition Test with 5 minutes break in between familiarization and novelty testing. Time (s) male mice injected with the indicated rAAV (mCherry-P2A-hpCTL (n=9), mCherry-P2A-hp708 (n12), or Nnat-P2A-hp708 (n=12)) explored either the familiar (F) or novel (N) object. Data are represented as box plot with whiskers and data points (+: mean, line: median; whiskers: minimum and maximum values). Two-way RM ANOVA: Novelty x Group, ****, p<0.0001; Novelty, ****, p<0.0001; Group, ns, p=0.5765. Šídák's post hoc test, F vs N: mCherry-P2A-hpCTL, ****, p<0.0001; mCherry-P2A-hp708, ns, p=0.6534; Nnat-P2A-hp708, ****, p<0.0001.

E. Tail Suspension Test. Time (s) male mice injected with the indicated rAAV (mCherry-P2A-hpCTL (n=9), mCherry-P2A-hp708 (n12), or Nnat-P2A-hp708

(n=12)) spent immobile. One-way ANOVA, Post hoc Tukey's Test: mCherry-P2A-hpCTL vs mCherry-P2A-hp708: ****, p<0.0001, mCherry-P2A-hpCTL vs Nnat-P2A-hp708: ns, p=0.9617, mCherry-P2A-hp708 vs Nnat-P2A-hp708: ****, p<0.0001. Data are represented as box plot with whiskers and data points (+: mean, line: median; whiskers: minimum and maximum values).

Table 1.

	Control	**BD**	**MDD**	**P Value**
n (f/m)	26/31	26/37	18/24	N/A
Age ± *S.D.*	29.4 ± 5.4/ 39.7± 13.4	29.9 ± 5.4/ 41.7 ± 11.3	29.6± 4.9/ 39.3.6± 14.7	0.94/0.75
CTQ ± *S.D.* (%)	40.7 ± 11.4 (53.8%)	42.3 ± 13.2 (30.8%)	50.2 ± 20.2 (61%)	0.1067/0.4170
Family history of MDs (%)	8 (30.8%)/ 5 (16.1%)	10 (38.5%)/ 10 (27.0%)	5 (27.8%)/ 7 (29.1%)	N/A
HAMD ± *S.D.*	2.7 ± 3.9/ 1.5 ± 2.5	7.5 ± 6.2/ 8.6 ± 6.4	14.8 ± 6.7/ 10.3 ± 7.7	<0.0001
YMRS ± *S.D.*	0.5 ± 1.1/ 0.7 ± 1.7	2.4 ± 2.9/ 7.0 ± 8.2	1.4 ± 1.6/ 1.7 ± 2.2	<0.01/ <0.0001
BDI ± *S.D.*	6.1 ± 6.1/ 4.5 ± 3.9	12.9 ± 11.1/ 12.9 ±9.6	26.6 ± 11.0/ 16.6 ± 10.7	<0.0001
AD (%)	0 (0%)	7 (26.9%)/ 17 (45.95%)	16 (88.9%)/ 17 (70.83%)	N/A
Antipsychotic (%)	0 (0%)	12 (46.15%)/ 19 (51.35%)	7 (38.89%)/ 4 (16.67%)	N/A
Lithium (%)	0 (0%)	4 (15.38%)/ 12 (32.43%)	1 (5.56%)/ 0 (0%)	N/A
Anticonvulsive (%)	0 (0%)	6 (23.08%)/ 10 (27.03%)	1 (5.56%)/ 1 (4.17%)	N/A
Stimulants (%)	0 (0%)	0 (0%)/ 1 (2.70%)	0 (0%)/ 2 (8.33%)	N/A

Benzodiazepine (%)	0 (0%)	0 (0%)	1 (5.56%)/ 0 (0%)	N/A
Z substance (%)	0 (0%)	0 (0%)/ 1 (2.70%)	1 (5.56%)	N/A

Subjects for miR-708-5p expression analysis on psychiatrically healthy controls (Control), Bipolar disorder patients (BD) or Major Depressive Disorder patients (MDD). One-way-ANOVA was performed to evaluate significant differences between groups. S.D.: standard deviation, CTQ: Childhood Maltreatment Questionnaire, HAMD: Hamilton Depression Rating Scale, YMRS: Young Mania Rating Scale, BDI: Beck's Depression Inventory, AD: antidepressant use.

Figures

Fig. 1 miR-708-5p is upregulated in the peripheral blood of human subjects at risk for or diagnosed with MDs.

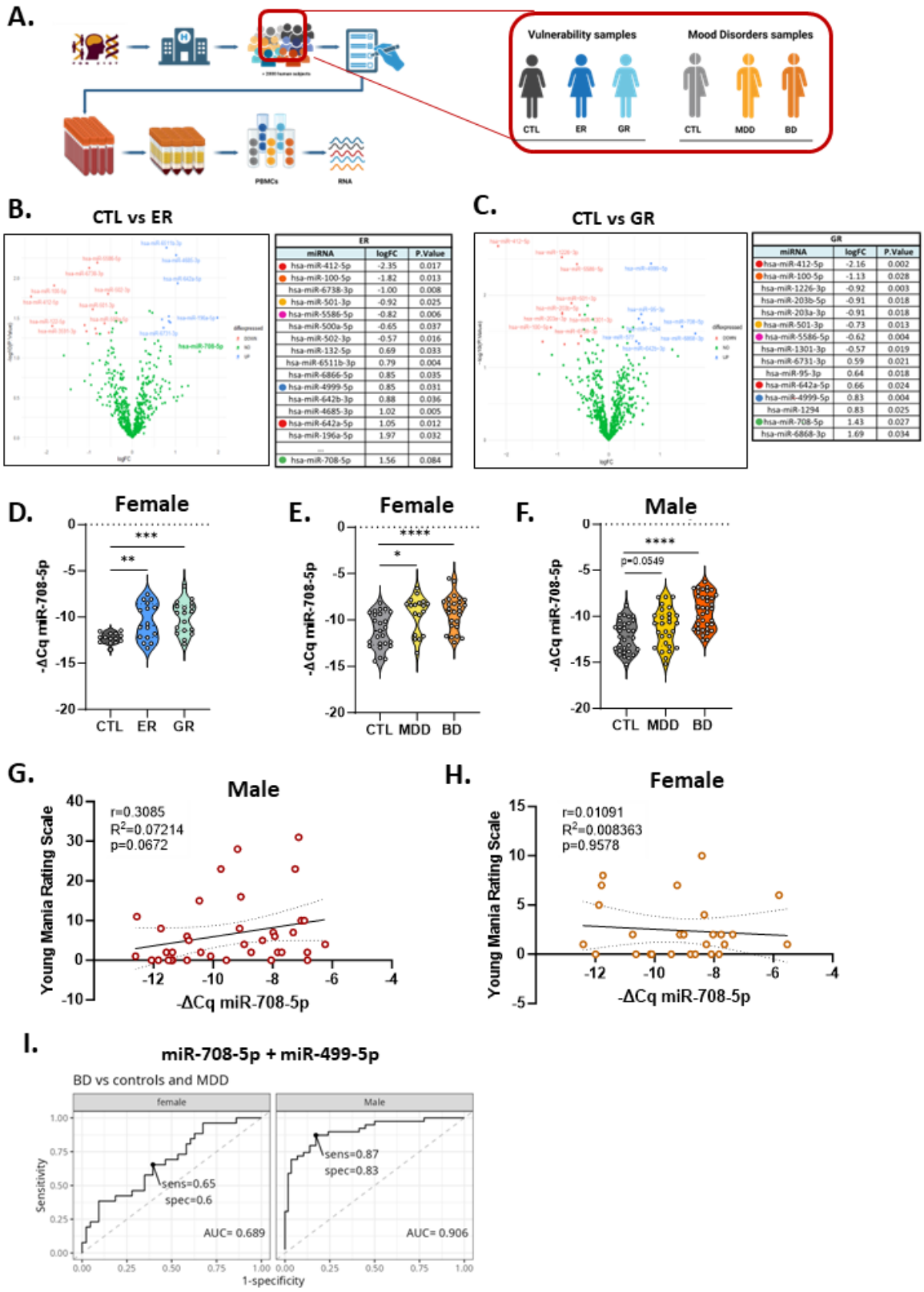

ER		
miRNA	logFC	P.Value
hsa-miR-412-5p	-2.35	0.017
hsa-miR-100-5p	-1.82	0.013
hsa-miR-6738-3p	-1.00	0.008
hsa-miR-501-3p	-0.92	0.025
hsa-miR-5586-5p	-0.82	0.006
hsa-miR-500a-5p	-0.65	0.037
hsa-miR-502-3p	-0.57	0.016
hsa-miR-132-5p	0.69	0.033
hsa-miR-6511b-3p	0.79	0.004
hsa-miR-6866-5p	0.85	0.035
hsa-miR-4999-5p	0.85	0.031
hsa-miR-642b-3p	0.88	0.036
hsa-miR-4685-3p	1.02	0.005
hsa-miR-642a-5p	1.05	0.012
hsa-miR-196a-5p	1.97	0.032
...		
hsa-miR-708-5p	1.56	0.084

GR		
miRNA	logFC	P.Value
hsa-miR-412-5p	-2.16	0.002
hsa-miR-100-5p	-1.13	0.028
hsa-miR-1226-3p	-0.92	0.003
hsa-miR-203b-5p	-0.91	0.018
hsa-miR-203a-3p	-0.91	0.018
hsa-miR-501-3p	-0.73	0.013
hsa-miR-5586-5p	-0.62	0.004
hsa-miR-1301-3p	-0.57	0.019
hsa-miR-6731-3p	0.59	0.021
hsa-miR-95-3p	0.64	0.018
hsa-miR-642a-5p	0.66	0.024
hsa-miR-4999-5p	0.83	0.004
hsa-miR-1294	0.83	0.025
hsa-miR-708-5p	1.43	0.027
hsa-miR-6868-3p	1.69	0.034

Figure 2. miR-708-5p is expressed in rat hippocampal neurons and upregulated in the hippocampus of rat models of environmental or genetic risk for MDs.

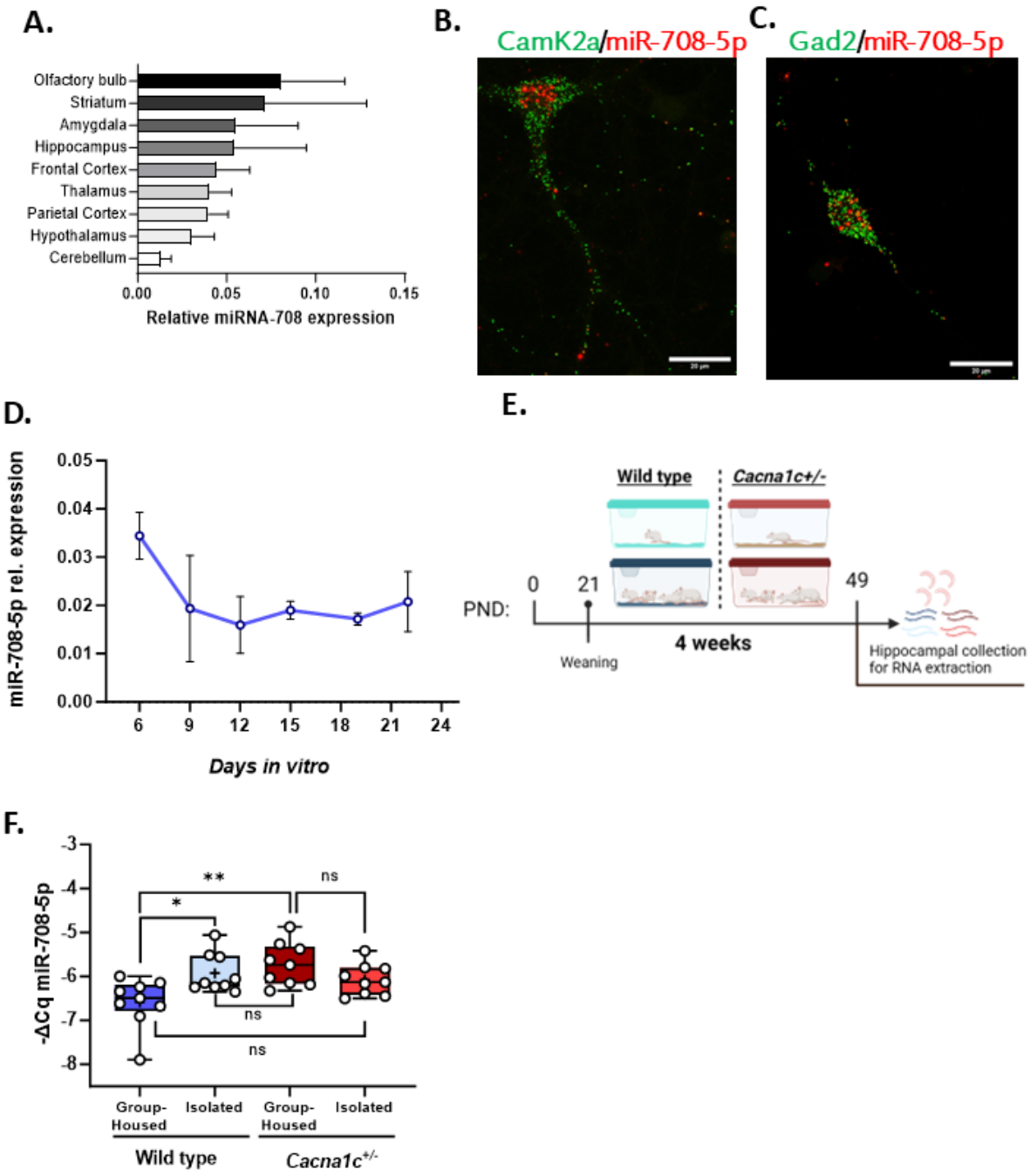

Figure 3. miR-708-5p overexpression in the mouse hippocampus recapitulates BD-associated endophenotypes.

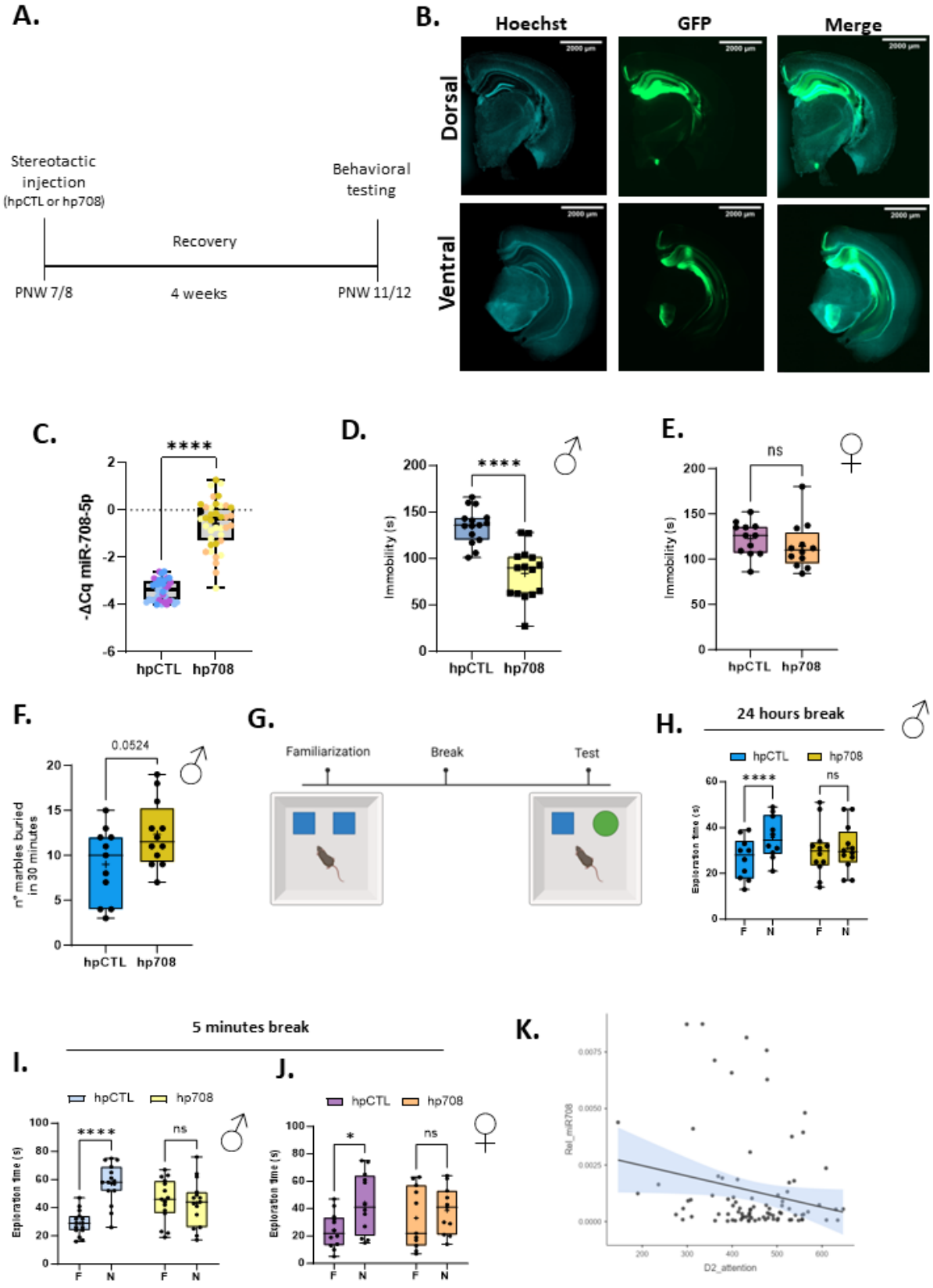

Figure 4. miR-708-5p directly targets Neuronatin (Nnat), an ER-resident protein involved in calcium homeostasis.

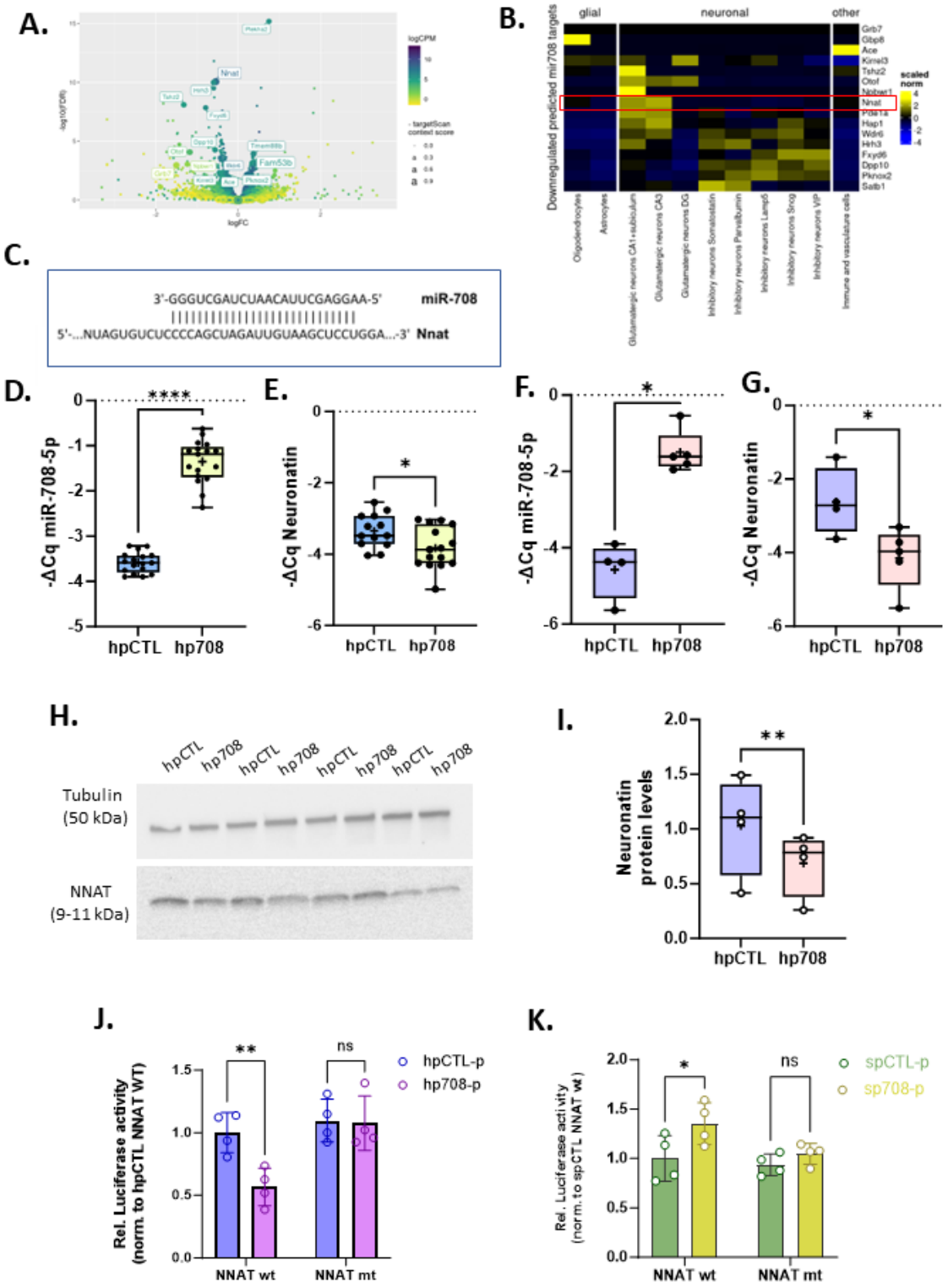
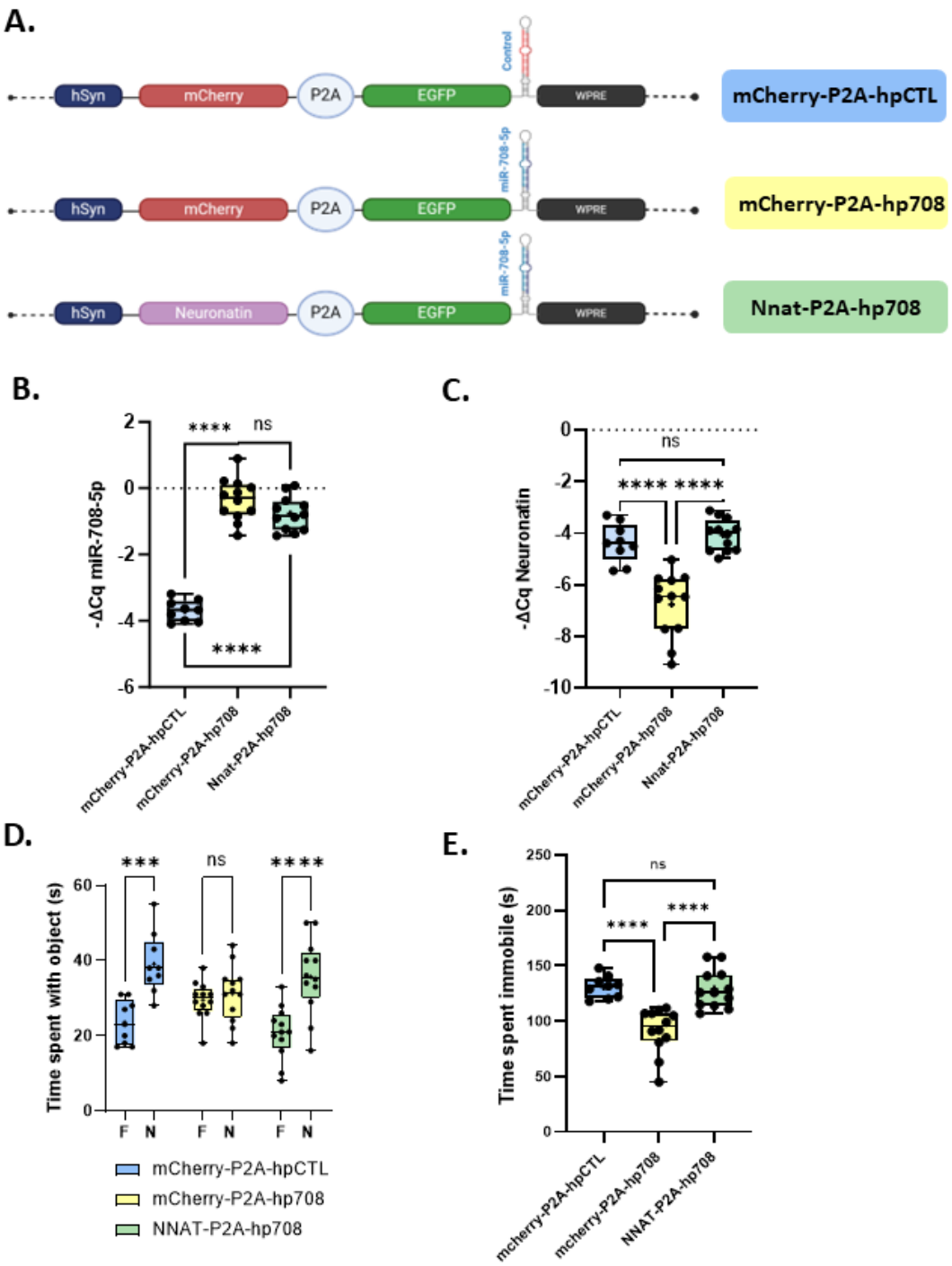
Figure 5. Restoring Nnat expression in miR-708-5p overexpressing hippocampal neurons rescues BD-associated behavior in mice.